

Review

Open Access



# Multi-interface engineering of nickel-based electrocatalysts for alkaline hydrogen evolution reaction

Xiaoxiang Zhang<sup>1,2</sup>, Yuxuan Guo<sup>1,2</sup>, Congwei Wang<sup>1,2,\*</sup>

<sup>1</sup>CAS Key Laboratory of Carbon Materials, Institute of Coal Chemistry, Chinese Academy of Sciences, Taiyuan 030001, Shanxi, China.

<sup>2</sup>Center of Materials Science and Optoelectronics Engineering, University of Chinese Academy of Sciences, Beijing 100049, China.

\*Correspondence to: Prof. Congwei Wang, CAS Key Laboratory of Carbon Materials, Institute of Coal Chemistry, Chinese Academy of Sciences, No. 27 Taoyuan South Road, Taiyuan 030001, Shanxi, China. E-mail: wangcongwei@sxicc.ac.cn

**How to cite this article:** Zhang X, Guo Y, Wang C. Multi-interface engineering of nickel-based electrocatalysts for alkaline hydrogen evolution reaction. *Energy Mater* 2024;4:400044. <https://dx.doi.org/10.20517/energymater.2023.115>

**Received:** 25 Dec 2023 **First Decision:** 20 Mar 2024 **Revised:** 16 Apr 2024 **Accepted:** 26 Apr 2024 **Published:** 15 May 2024

**Academic Editors:** Nicolas Alonso-Vante, Yun Zhang **Copy Editor:** Fangling Lan **Production Editor:** Fangling Lan

## Abstract

High gravimetric energy density and zero carbon emission of hydrogen have motivated hydrogen energy to be an attractive alternative to fossil fuels. Electrochemical water splitting in alkaline medium, driven by green electricity from renewable sources, has been mentioned as a potential solution for sustainable hydrogen production. Hydrogen evolution reaction (HER), as a cathodic half-reaction of water splitting, requires additional overpotential to obtain protons via water adsorption/dissociation, suffering from slow kinetics in alkaline solution. Robust and active nickel (Ni)-based electrocatalyst is a promising candidate for achieving precious-metal comparable performance owing to its platinum-like electronic structures with more efficient electrical power consumption. Various modification strategies have been explored on Ni-based catalysts, among which multi-interface engineering is one of the most effective routines to optimize both the intrinsic activity of Ni-based electrocatalysts and the extrinsic stacked component limitations. Herein, we systematically summarize the recent progress of multi-interface engineering of Ni-based electrocatalysts to improve their alkaline HER catalytic activity. The origin of sluggish alkaline HER kinetics is first discussed. Subsequently, three kinds of interfaces, geometrically and reactively, conductive substrate/electrocatalyst interface, electrocatalyst internal heterointerface, and electrocatalyst/electrolyte interface, were cataloged and discussed on their contribution mechanisms toward alkaline HER. Particular focuses lie on the microstructural and electronic modulation of key intermediates with energetically favorable adsorption/desorption behaviors via rationally designed interfaces. Finally, challenges and



© The Author(s) 2024. **Open Access** This article is licensed under a Creative Commons Attribution 4.0 International License (<https://creativecommons.org/licenses/by/4.0/>), which permits unrestricted use, sharing, adaptation, distribution and reproduction in any medium or format, for any purpose, even commercially, as long as you give appropriate credit to the original author(s) and the source, provide a link to the Creative Commons license, and indicate if changes were made.



perspectives for multi-interface engineering are discussed. We hope that this review will be inspiring and beneficial for the exploration of efficient Ni-based electrocatalysts for alkaline water electrolysis.

**Keywords:** Interface, electrocatalyst, alkaline, hydrogen evolution reaction

## INTRODUCTION

The scalable and sustainable production of hydrogen is essential to alleviating the environmental and energy crises<sup>[1-5]</sup>. In addition to holding a significantly higher energy density than conventional fossil fuels, hydrogen emits no greenhouse gases, endowing it as a cleaner energy source<sup>[6]</sup>. In light of these characteristics, it offers a vast range of applications in smart grids, residential heating systems, hydrogen vehicles, and fuel cell systems. Currently, coal gasification and steam reforming account for more than 96% of the world's annual hydrogen output, during which excessive energy would be consumed and vast amounts of greenhouse gases would be inevitably released into the atmosphere<sup>[7,8]</sup>. Therefore, it is attractive and desirable to upgrade the hydrogen production method from conventional techniques to the innovative technology, e.g., ion exchange membrane-based water electrolysis, to further fulfill the ambitious carbon neutral goals and facilitate the transition toward low-carbon power systems<sup>[9]</sup>. Specifically, the proton exchange membrane (PEM) can be assembled into membrane electrode assemblies (MEAs) as a water electrolyzer to directly produce high-purity hydrogen from water. More significantly, PEM could be further coupled with renewable and intermittent energy (solar, wind, tidal, *etc.*) to store the energy/electricity into chemical forms and integrated within the power grid (acting as load) to relieve network bottlenecks with improved system flexibility<sup>[10]</sup>. Despite these unique benefits, the practical applications of these devices face obstacles due to the expensive electrolyte-tolerant parts and catalysts. Typically, precious metal (oxides)-based catalysts and titanium alloy/stainless-steel components are essential for the stable operation of PEM electrolyzers in acidic medium. Comparatively, an anion exchange membrane (AEM) electrolyzer, in which alkaline electrolyte is employed as the ion diffusion and reactive media, can introduce earth-abundant metals (Ni/Co/Fe, *etc.*) as catalyst materials, enabling promising application perspectives with great advantages than PEM electrolyzers<sup>[11]</sup>. Nevertheless, the unsatisfactory performance of these non-precious metal catalysts generally results in high energy barriers and low energy efficiency. Consequently, the pursuit of cost-effective, reliable, and high-performing catalysts has emerged as a significant research frontier for alkaline water splitting technology<sup>[12,13]</sup>.

Principally, electrocatalytic water splitting includes hydrogen evolution reaction (HER) for the cathode and oxygen evolution reaction (OER) for the anode, respectively<sup>[14]</sup>. Unlike the abundant protons supplied in acidic electrolyte, the HER undergoes a sequential two-step process in alkaline conditions, during which the protons are generated via the water dissociation firstly and transformed into hydrogen molecular subsequently<sup>[15,16]</sup>. This additional water adsorption/dissociation step in alkaline electrolyte accounts for more than 2-3 orders of magnitude slower kinetics than that of acidic conditions<sup>[17,18]</sup>. Moreover, the inclusion of extra steps would also result in extra energy consumption, defined as the overpotentials beyond the thermodynamic energy. Therefore, the advancement of electrocatalysts is crucial in order to diminish these excessive overpotentials and accelerate the reaction kinetics<sup>[19]</sup>. It is widely acknowledged that platinum (Pt)-based materials have the best HER electrocatalytic performance<sup>[20,21]</sup>. However, their application is hindered by the high cost and scarce storage<sup>[22]</sup>. In order to address these issues, earth-abundant non-precious metal materials have triggered extensive attention, among which nickel (Ni)-based materials have exhibited great potentials owing to their earth abundance, cost-effectiveness, and, most importantly, holding similar electronic properties to Pt<sup>[23]</sup>. Unfortunately, Ni-based electrocatalysts currently still cannot completely replace Pt due to their relatively strong H adsorption, insufficient active sites, and high energy barriers for water adsorption/dissociation in alkaline conditions, which hampered their

practical application. Therefore, the dilemma of conventional Ni-based catalysts lies in that the sole Ni content cannot simultaneously promote the water dissociation and the desorption of adsorbed hydrogen intermediate ( $H_{ad}$ ) in alkaline medium, not to mention the potential modulation of hydroxy groups. Therefore, rationally designing and fabricating Ni-based electrocatalysts with excellent intrinsic activity is still a grand challenge at present<sup>[24]</sup>.

During the last decade, growing interests have been attracted in the construction of multi-component composite systems to intentionally overcome the limitations of sole Ni catalyst via different strategies, e.g., (Ni) metal alloying/dealloying<sup>[25-27]</sup>, heteroatom doping<sup>[28-30]</sup>, strain engineering<sup>[31-33]</sup>, multi-interface engineering<sup>[34-38]</sup>, *etc.* Among them, the multi-interface engineering has exhibited substantial potential to synergistically optimize the entire HER systems from different perspectives: geometrically and chronologically, three interfaces, including (1) conductive substrate/electrocatalyst interface; (2) internal interface of electrocatalyst; and (3) electrocatalyst/electrolyte interface, could be optimized to fundamentally facilitate the alkaline HER performance. Specifically, close and flawless contact between the conductive substrate and electrocatalyst could effectively minimize the charge transfer resistance and benefit the HER kinetics with smaller overpotential. Secondly, multi-component Ni-based catalysts with wisely heterointerface engineering (e.g., ensemble effect and electronic modulation) enable the optimization of both the thermodynamics and kinetics of HER processes. Thirdly, a robust electrocatalyst/electrolyte interface is significant for achieving a stable HER performance, particularly for high current density conditions. The generated gas bubbles could induce great inner pressure at the interface and lead to severe catalyst damage or structure failure. During high current density and prolonged operation, the accumulation of bubbles and generation of joule heat can cause the electrocatalyst to easily detach from the conductive substrate. By optimizing the substrate/electrocatalyst interface, the binding strength between the electrocatalyst and the substrate can be enhanced, resulting in improved stability of the electrocatalyst. By introducing defect sites or constructing heterostructures to optimize the internal interface of electrocatalyst, the intrinsic catalytic activity of the electrocatalyst can be enhanced, leading to higher conversion efficiency of reactant species and promoting long-term stable operation of the electrocatalyst. Additionally, by adjusting the wettability of electrocatalyst/electrolyte interface, the wetting properties of the electrolyte and the bubble detachment rate can be improved, allowing the electrocatalyst to exhibit superior performance during prolonged catalytic processes. Therefore, reasonable multi-interface design can significantly break the activity limitation of electrocatalysts.

Recent advances of interface engineering for alkaline HER electrocatalysts have been summarized in several reviews. Xu *et al.* thoroughly summarized the atomic heterointerface engineering for improving the catalytic performance of electrocatalysts<sup>[39]</sup>. Wei *et al.* focused on the advances in building heterostructured catalysts for accelerating the Volmer step in alkaline conditions<sup>[40]</sup>. Huang *et al.* discussed a series of representative heteroatom-modified electrocatalysts with properly designed multi-component interfaces and highlighted the optimized HER reaction pathway<sup>[41]</sup>. These reviews mostly focus on the interface engineering of the electrocatalyst itself, whereas the other two types of interface with both conductive substrate and electrolyte still lack detailed discussion, especially based on the electrocatalytic HER mechanism. Herein, the multi-component functions, design protocols and synthesis approaches of multi-interface engineering are summarized and discussed for exploring efficient Ni-based alkaline HER electrocatalysts [Figure 1]. We first summed up the alkaline HER mechanism, the origin of the sluggish kinetics for elementary steps, and the critical electrochemical parameters to evaluate the HER performance. Afterward, detailed discussions on the aforementioned three types of interfaces are organized, focusing on the internal interface of electrocatalyst to modulate the HER elementary process thermodynamically and kinetically. Finally, the challenges and prospects of multi-interface engineering for the design of alkaline HER electrocatalysts are discussed.

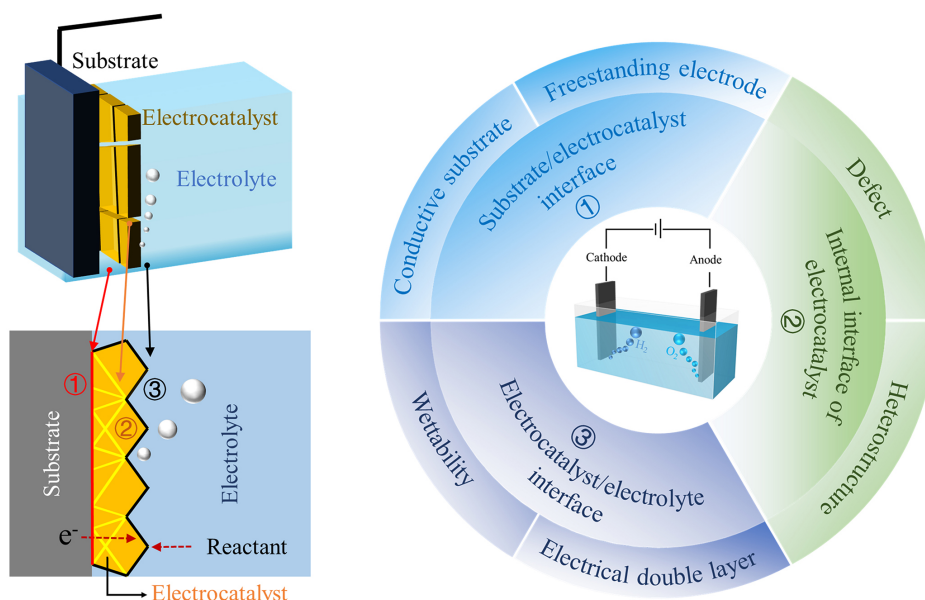


**Figure 1.** Schematic illustration of multi-interface structure and engineering strategies.

## FUNDAMENTAL MECHANISMS OF ALKALINE HER

A typical water electrolyzer consists of three stacked components: a cathode, an anode, and an electrolyte. Two half reactions, HER and OER, occur at the cathode and anode, respectively. Although the reaction of splitting water into hydrogen and oxygen was discovered in acidic electrolyte, the water splitting in alkaline electrolyte has been commercialized on a large scale for a century owing to its more economic efficiency with robust electrocatalysts. The cathodic HER is recognized as a relatively basic catalytic reaction involving a two-electron transfer process, which could be divided into two elementary steps regardless of whether it occurs in acidic or alkaline electrolyte: (i) hydrogen adsorption step (Volmer step), during which a proton ( $H^+$ ) combines an electron on the active sites to generate an adsorbed hydrogen intermediate; (ii) hydrogen desorption step (Heyrovsky/Tafel step), during which the obtained  $H_{ad}$  would form hydrogen molecule and desorb from the catalyst surface via either Heyrovsky or Tafel step. The detailed HER process is illustrated as the following elementary steps [Figure 2].

For acidic HER, the generation of hydrogen molecules is associated with the hydrogen adsorption free energy ( $\Delta G_H$ ) on the active sites. The well-established Sabatier principle indicates that the interaction between an optimal catalyst and the reactive intermediates should not be too strong or weak. Therefore,  $\Delta G_H$  has been widely accepted as a descriptor for the acidic HER. However, unlike acidic electrolyte containing a large number of available protons, alkaline HER needs to first adsorb water molecules and then overcome additional energy barriers to dissociate the water to produce protons. Therefore, the Volmer step in alkaline medium is controlled not only by  $\Delta G_H$  but also determined by the adsorption and dissociation energy barriers of  $H_2O$  molecules. Moreover, the adsorption/desorption behavior of accompanied hydroxyl groups ( $OH_{ad}$  and  $OH^-$ ) would also bring complexity for the overall reaction efficiencies. A delicate balance between these determinants needs to be optimized to achieve an efficient alkaline HER performance. Too weak water molecule adsorption strength could not generate sufficient reactants, while too strong  $H_{ad}/OH_{ad}$  adsorption strength would result in a poisoning effect as the surface-active sites would be overly occupied.



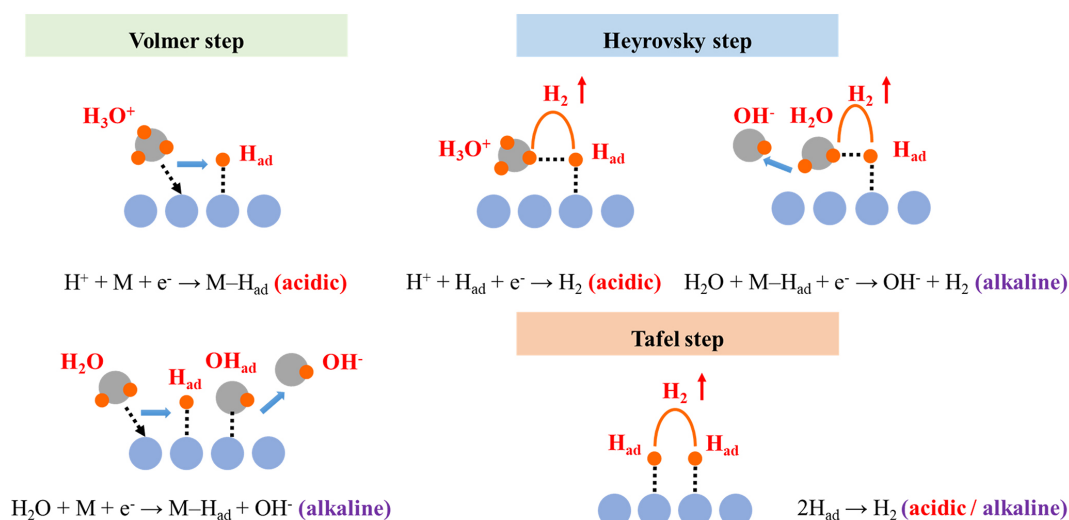


**Figure 2.** Schematic illustration for the elementary HER step: Volmer step and Heyrovsky step/Tafel step. balls in blue: active sites; grey: O atom; orange: H atom, respectively.

## ELECTROCHEMICAL PARAMETERS OF HER

The performance of a given HER electrocatalyst is commonly assessed using a few key electrochemical parameters, including overpotential ( $\eta$ ), Tafel plot, electrochemical impedance spectroscopy (EIS), turnover frequency (TOF), stability, *etc.* Through these parameters, the detailed reaction thermodynamics and kinetics information could be extracted. In this section, a concise overview of these parameters will be provided.

### Overpotential

The representative polarization curves are obtained by graphing the geometric current density against the applied potential. The  $\eta$  is described as the potential gap between the actual applied potential for triggering the reaction and the thermodynamic equilibrium potential. A larger  $\eta$  indicates an increased electricity consumption, thereby resulting in a limited energy conversion efficiency. A satisfactory electrocatalyst should exhibit a higher current density at a low overpotential. Nernst equation elucidates the relationship between the HER equilibrium potential ( $E_{\text{HER}}$ ) and the standard hydrogen electrode potential ( $E_{\text{SHE}}$ ) which is defined as 0 V at any temperature.

$$E_{\text{HER}} = E_{\text{SHE}} + \frac{RT}{zF} \times \ln \frac{\alpha_{\text{H}^+}^2}{p_{\text{H}_2}} \quad (1)$$

$$E_{\text{HER}} = 0.059 \times \text{pH} \quad (2)$$

$$E = E_{\text{HER}} + \eta \quad (3)$$

where  $R$  is the gas constant,  $T$  represents the temperature in kelvins,  $z$  denotes the number of electrons transferred ( $z = 2$  for HER),  $F$  is the Faraday constant ( $96,485 \text{ C mol}^{-1}$ ),  $\alpha_{\text{H}^+}$  depicts the activity of  $\text{H}^+$  in aqueous solution, and  $p_{\text{H}_2}$  is the partial pressure of  $\text{H}_2$  (Eq. 1). In the certain condition ( $T = 298 \text{ K}$ , unit  $\text{H}_2$  partial pressure),  $E_{\text{HER}}$  can be considered as reversible hydrogen electrode (RHE) which also depends on pH values (Eq. 2). Therefore, the actual applied potential ( $E$ ) equals to  $E_{\text{HER}}$  plus  $\eta$  (Eq. 3).

The origins of  $\eta$  include the activation barriers of electrochemical reactions, ion migration, and internal resistance of the measurement system ( $R_s$ ). An excellent catalyst can reduce the activation energy barriers required for initiating the reaction. Ion migration and series resistances are mostly dependent on external testing system configurations. The ohmic potential drop caused by  $R_s$  can be corrected by iR compensation. Therefore, the terminal  $E$  can be given by

$$E = E_{HER} + \eta - iR_s \quad (4)$$

Generally, the overpotential needed to achieve a current density of 10 mA cm<sup>-2</sup> (geometric current density) ( $\eta_{10}$ ) has been widely accepted as a criterion for evaluating the catalytic activities of different HER electrocatalysts. This current density corresponds to a 12.3% solar-to-fuel efficiency in solar water splitting. Essentially, owing to the different loading masses and accessible active areas for catalysts prepared via various methods,  $\eta_{10}$  based on geometric area is not suitable to evaluate the intrinsic activity of HER electrocatalysts. Therefore, the specific activity (based on real surface area) is proposed to measure the catalyst activity, which can be calculated by normalizing the current to the Brunauer-Emmett-Teller (BET) surface area or the electrochemical surface area (ECSA).

### Tafel plot

Tafel plot can be well employed to investigate the inherent kinetics information of the electrocatalyst, which is derived from the experimentally measured polarization curves. When the solution concentration at the electrode surface is comparable to that of the bulk solution, the overpotential connected with the electrode kinetics can be significantly correlated with the current density by the Butler-Volmer equation, denoted as

$$i = i_0 [e^{\alpha f \eta} - e^{-(1-\alpha) f \eta}] \quad (5)$$

where  $i$  represents the current density,  $i_0$  is the exchange current density under reversible conditions,  $\alpha$  is the charge transfer coefficient, and  $f$  equals to  $F/RT$ . In the region of high overpotential, Eq. 5 can be simplified to

$$\eta = -\left(\frac{2.303RT}{\alpha F}\right) \log i_0 + \left(\frac{2.303RT}{\alpha F}\right) \log i \quad (6)$$

According to Eq. 6, the relationship between overpotential and Tafel slope ( $b$ ) can be expressed as

$$\eta = b \log(|i/i_0|) \quad (7)$$

where  $i_0$  is the rate of charges entering or leaving the electrocatalyst surface under reversible conditions in an electrolyte, which can be extracted at the overpotential of zero. A high  $i_0$  indicates the easier polarization of the electrocatalyst, and a lower activation overpotential to trigger the electrode reaction. The possible reaction mechanisms can be inferred from the value of the Tafel slope. For example, the Tafel slope of  $b > 120$ ,  $40 \leq b \leq 120$  or  $b < 40$  mV dec<sup>-1</sup> indicates that the Volmer, Heyrovsky, or Tafel step could be the HER rate-determining step (RDS), respectively. An electrocatalyst with a high  $i_0$  and a low Tafel slope has always been an attractive proposition.

### Charge transfer resistance

For an electrochemical reaction, the charge transfer characteristics are an important descriptor of an electrocatalyst activity, which can be evaluated from the EIS measurement technique within a reasonable frequency band. Generally, EIS measurements are conducted at the amplitude of perturbation voltage of 5-10 mV and over an applied potential beyond onset potential (at this potential, the catalysts should exhibit appreciable activity). The charge transfer resistance can provide information about the charge transfer process, which significantly depends on the analyzed frequency range. Specifically, (i) the resistance at the high-frequency region is independent of the applied potential owing to the non-faradic process, which can be employed to evaluate the resistances between electrode and catalyst; (ii) the resistance at the medium-frequency region is usually employed to reflect the charge transport within the catalyst; and (iii) the resistance at the low-frequency region is used to study the charge transfer resistance ( $R_{ct}$ ) of interfacial charge transfer between the electrocatalyst and the solution. When the reaction current is not controlled by the mass-transfer resistance and at low overpotentials,  $R_{ct}$  can be expressed as

$$R_{ct} = \frac{RT}{nFi_0} \quad (8)$$

where  $n$  is the number of transferred electrons. Smaller values of  $R_{ct}$  indicate faster reaction kinetics and potentially better catalytic performance.

### Turnover frequency

TOF is defined as the number of the desired product per active site in unit time (second, Eq. 9) at a predefined applied potential, which is an important parameter for measuring the intrinsic activity of an electrocatalyst. Nevertheless, the exact value of TOF is difficult to measure because the actual population of active sites cannot be accurately determined for heterogeneous catalysis. In some instances, the TOF can be obtained by calculating the total catalyst loadings, no matter whether they are truly involved in the catalytic process. In other cases, many researchers reported that the sole surface atoms or the easily accessible surface catalytic sites of the electrocatalysts participate in the catalytic process and generated the TOFs accordingly. Nonetheless, such results are meaningful when similar electrocatalysts are compared.

$$\text{TOF} = \frac{n_{\text{product}}}{n_{\text{active sites}} \times t} \quad (9)$$

For HER, assuming that Faradaic efficiency is 100%, and the number of  $\text{H}_2$  can be expressed as

$$n_{\text{H}_2} = \frac{It}{zF} \quad (10)$$

Consequently, Eq. 10 can be simplified to

$$\text{TOF} = \frac{I \times N_A}{z \times n_{\text{active sites}} \times F} \quad (11)$$

where  $I$  is current (A),  $z$  represents the quantity of electron transferred per molecule ( $z = 2$ , for HER), and  $N_A$  denotes the Avogadro number ( $6.022 \times 10^{23}$ ).

## Stability

Besides the intrinsic activity, the time-dependent stability is also a very important parameter for potential applications, especially under high current conditions. Two approaches exist for evaluating the durability of an HER electrocatalyst, including the chronopotentiometry (CP)/chronoamperometry (CA) and accelerated cyclic voltammetry (CV) tests. CP/CA test is conducted by recording the curve of potential/current over time under a fixed current/potential, respectively. For CP or CA test, most reported works are performed at a current density lower than  $200 \text{ mA cm}^{-2}$ . In fact, for practical application, durability test at higher current densities is encouraged for mimicking the real working conditions in AEM. In CV test, generally, larger than 1,000 CV cycles are repeated by recording the potential with the current response. By comparing the polarization curves before and after CV cycles, it can be seen that the less  $\eta$  increment, the better the stability of the electrocatalysts.

## MULTI-INTERFACE ENGINEERING OF ALKALINE HER ELECTROCATALYSTS

For a complete electrocatalytic HER process, electrons from the external power source would structurally and chronologically go across three interfaces to reach the active site and participate in the reaction, including conductive substrate/electrocatalyst, electrocatalyst internal and electrocatalyst/electrolyte interfaces. Therefore, engineering these multi-interfaces is very important to optimize the overall electrocatalytic performance, which will be meticulously reviewed in this section.

### Conductive substrate/electrocatalyst interface

In order to enhance electron transport efficiency with minimal charge resistance and avoid the electroheat energy waste, a geometric and electric close interfacial contact between an active electrocatalyst and a conductive substrate is essential. Most commercial and experimental electrodes are currently made by coating active catalyst materials onto a conductive substrate with the assistance of polymer binders, inevitably resulting in a vulnerable interfacial adhesion and hindrance to electron transport. In order to strengthen this interface, *in-situ* synthesizing catalytically active materials on conductive substrates or directly preparing self-supported freestanding electrode/electrocatalyst has been documented to address these interface issues.

#### *Conductive substrate*

The commonly used conductive substrates mainly include nickel (NF)/copper foam, Ni-based alloy foam, carbon cloth, carbon paper, *etc.*, among which the NF has been reported as the most popular electrode substrate. On the choice of the conductive substrate, NF has enjoyed widespread application as its distinctive interlinked third-dimensional (3D) microstructure provides merits as light weight, high porosity, reliable mechanical strength, chemical stability, and promising electrical conductivity. Moreover, its employment could also act as the nickel source during the synthesis, offering further opportunities for constructing Ni-based compounds with multi-interface. For example, through a two-step synthetic procedure, specifically, the 1st step preparation of  $\text{NiMoO}_4 \cdot x\text{H}_2\text{O}$  nanowire arrays followed by the 2nd step pyrolysis process, Liu *et al.* constructed  $\text{MoO}_2$ -Ni nanowire arrays supported on NF as an efficient HER catalyst [Figure 3A-J]. Benefiting from the *in-situ* grown  $\text{MoO}_2$ -Ni heterostructure with an atomically infused interface, the HER kinetics was enhanced by the upraised atomic  $d$  orbital<sup>[42]</sup>. The optimized  $\text{MoO}_2$ -Ni@NF electrocatalyst exhibited exceptional Pt-like HER performance in 1 M KOH<sup>[42]</sup>. Chang *et al.* electrodeposited amorphous Ni-Co-Fe ternary phosphides ( $\text{Ni}_4\text{Co}_4\text{Fe}_1\text{-P}$ ) on NF as a self-supported catalytic electrode for alkaline HER. The integration of multimetallic phosphide on the NF surface allows sufficient exposure of surface sites<sup>[43]</sup>. Therefore, the  $\text{Ni}_4\text{Co}_4\text{Fe}_1\text{-P}$  electrode presented good HER catalytic performance ( $-61 \text{ mV}$  at  $-20 \text{ mA cm}^{-2}$ )<sup>[43]</sup>. Ni-Cu-P@Ni-Cu catalyst was also prepared using electrodeposition as an efficient electrode for HER. During electrodeposition, NF provided sufficient active sites for the growth of dendrites with unique structures. Its high active electrochemical area, the convenient mass transfer channels

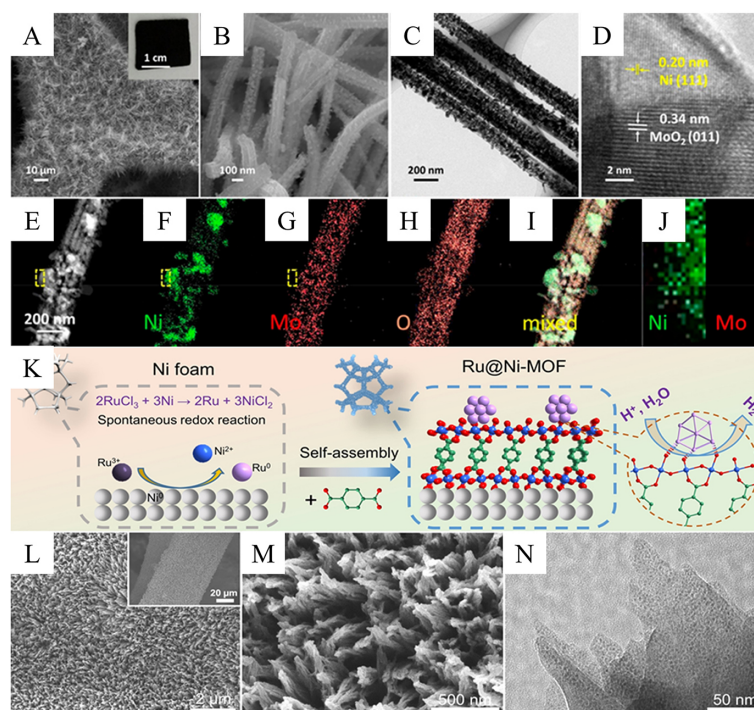


**Figure 3.** (A and B) SEM images of MoO<sub>2</sub>-Ni on NF. (C) TEM, (D) HRTEM, (E-J) HAADF-STEM images and elemental analysis results of MoO<sub>2</sub>-Ni nanowires. (K) Schematic illustration of the formation of Ru@Ni-MOF grown on NF. (L, M) SEM and (N) TEM images of Ru@Ni-MOF. This figure is quoted with permission from Liu *et al.*<sup>[42]</sup> and Deng *et al.*<sup>[45]</sup>.

provided by the porous structure, and the synergistic effect between Cu and Ni led to the excellent electrocatalytic activity ( $-70$  mV at  $10$  mA cm<sup>-2</sup>) of the catalyst<sup>[44]</sup>. Deng *et al.* designed a definite metal-support interfacial bond to enhance the intrinsic activity of noble metals (Ru, Ir, and Pd)<sup>[45]</sup>. Through a spontaneous redox strategy, three kinds of quantum-sized metal nanoparticles propped against Ni-based metal-organic framework (Ni-MOF) nanohybrids (Ru@Ni-MOF, Ir@Ni-MOF, and Pd@Ni-MOF) were rationally prepared. As shown in Figure 3K-N, Ru<sup>3+</sup> and metallic Ni on the NF surface spontaneously underwent a redox reaction, during which Ni<sup>2+</sup> ions were also coordinated with 1,4-benzenedicarboxylic acid (H<sub>2</sub>BDC) to shape Ni-MOF nanosheets. The scanning electron microscopy (SEM) and transmission electron microscopy (TEM) images demonstrated the uniform distribution of Ru nanoparticles anchored (2-4 nm) on the Ni-MOF surface. The strong interfacial interaction between the nanoparticles and Ni-MOF ensured not only the structural stability but also adequate exposure of active sites. More significantly, the electronic structure of hybrid materials was successfully modulated by the charge exchange in the formed Ni-O-M (Ru, Ir, Pd) bridge bond with enhanced HER kinetics. Consequently, the Ru@Ni-MOF catalyst exhibited superior HER performance, even superior to commercial Pt/C. Theoretical calculation demonstrated that the interfacial-bond-induced electron transfer resulted in the optimized adsorption of H<sub>2</sub>O and H leading to the excellent alkaline HER performance<sup>[45]</sup>. Electrochemical dealloying strategy was also used to prepare nickel nanotube arrays on NF and achieved a high HER kinetics<sup>[46]</sup>. Liang *et al.* synthesized MoO<sub>2</sub>/Ni heterostructure on NF by hydrothermal followed by pyrolysis in N<sub>2</sub> and H<sub>2</sub> atmosphere<sup>[47]</sup>. Firstly, using hydrothermal methods, the NiMoO<sub>4</sub>·xH<sub>2</sub>O nanosheet was formed on the NF surface, and then the NiMoO<sub>4</sub>·xH<sub>2</sub>O precursor transformed into MoO<sub>2</sub>/Ni under N<sub>2</sub> and H<sub>2</sub> atmosphere gas environments. The *in-situ* transformation of the precursor ensured the stability of the interface between the active site (MoO<sub>2</sub>/Ni) and the substrate (NF). Eventually, the MoO<sub>2</sub>/Ni@NF displayed robust HER performance in an alkaline electrolyte<sup>[47]</sup>. Similarly, Ni-doped tungsten oxide grown on NF catalyst



(Ni-WO<sub>x</sub>@NF) was also prepared by first hydrothermal and then annealing to produce hydrogen from seawater. The Ni-WO<sub>x</sub> catalyst grew vertically on the NF surface with rapid charge transfer and low  $\eta_{10}$  (45.69 mV)<sup>[48]</sup>. In addition, using one-step solvothermal method, the W-doped Ni-C<sub>3</sub>S<sub>3</sub>N<sub>3</sub>-based coordination polymer (CP) catalyst was also prepared on NF (W-NT@NF). The metal-organic polymers were grown in situ on NF with low interfacial resistance and a great many of exposed active sites, which achieved excellent dual-functional HER and urea oxidation reaction performance<sup>[49]</sup>. In the traditional thermocatalysis field, such as selective oxidation, hydrogenation or water-gas shift reaction, Ni/TiO<sub>2</sub> systems have proven to be good catalysts. However, their poor electrical conductivity limits their application in electrocatalysis. Zhou *et al.* synthesized Ni/TiO<sub>2</sub> composites on conductive NF as a HER electrode<sup>[50]</sup>. The disclosed electronic interaction between Ni and TiO<sub>2</sub>, coupled with excellent electrical conductivity of NF, endowed the composites with outstanding HER performance<sup>[50]</sup>.

Ni-based alloy foams could provide more growth sites when the conductive substrate is combined with active substance by hydrothermal methods. For instance, a HER electrocatalyst (NiFeCoS<sub>x</sub>@FeNi<sub>3</sub>) consisting of Co<sub>3</sub>S<sub>4</sub> and Ni-Fe sulfide on FeNi<sub>3</sub> foam was prepared. The synergistic interaction among multi-elements and the unique structure together gave the catalyst outstanding catalytic performance. In alkaline solution, the  $\eta_{10}$  of NiFeCoS<sub>x</sub>@FeNi<sub>3</sub> is 88 mV<sup>[51]</sup>. In addition to Ni-based conductive substrates, copper substrates could also serve as good conductive substrates. A dynamic hydrogen bubble template (DHBT) method is a practical approach to fabricating the porous alloy electrodes. The porous Ni-Co catalyst on a copper substrate electrode was prepared using the DHBT method and exhibited outstanding stability<sup>[52]</sup>. Zhang *et al.* prepared an efficient HER electrocatalyst by coating metallic Ni onto Cu<sub>2</sub>S nanoarrays using the commercial copper foam as a substrate and unveiled a preferable HER activity ( $\eta < 200$  mV at 500 mA cm<sup>-2</sup>). Finally, theoretical analyses indicated that the Ni-S interaction between metallic Ni and Cu<sub>2</sub>S interface can optimize the adsorption energy of hydrogen and thus promote HER kinetics<sup>[53]</sup>.

Moreover, carbon cloth has been widely used as a conductive substrate for HER because of its superior electric conductivity, low cost, and robust mechanical flexibility. Yang *et al.* prepared an electrocatalyst containing W<sub>2</sub>C nanowires decorated with Ni nanoparticles on carbon cloth<sup>[54]</sup>. It only required a low overpotential of 37 mV to obtain current densities of 10 mA cm<sup>-2</sup>, which was comparable to the commercial Pt/C catalyst. Moreover, the experimental results indicated that the close interaction between Ni nanoparticles and W<sub>2</sub>C nanowires can effectively accelerate electron transport<sup>[54]</sup>. A NiO/Ni heterostructure on carbon cloth (NiO/Ni@CC) was fabricated by *in-situ* electrochemical oxidation after electrodepositing metallic Ni on the surface of carbon cloth. The existence of heterostructure and the superior electric conductivity of carbon cloth made the catalyst exhibit a low  $\eta_{10}$  of 40 mV for alkaline HER<sup>[55]</sup>. Theoretical calculations by Wang *et al.* predicted that coupling Ni<sub>3</sub>C with metallic Ni can balance H and H<sub>2</sub>O adsorption energies. Subsequently, they fabricated an integrated heterostructure catalyst consisting of Ni<sub>3</sub>C nanosheets and Ni nanoparticles on carbon cloth, demonstrating excellent electrocatalytic HER activity ( $\eta_{10} = 98$  mV)<sup>[56]</sup>. Inspired by the distinctive water dissociation ability of V-O species, a novel Ni/V<sub>2</sub>O<sub>3</sub> heterostructure was prepared on carbon cloth and characterized as an alkaline HER electrocatalyst, an excellent HER activity of low overpotential ( $\eta_{10} = 44$  mV) was revealed<sup>[57]</sup>. Carbon microfibers derived from skim cotton were also introduced as conductive substrates for HER catalyst. Sun *et al.* synthesized Mo<sub>2</sub>C and metallic Ni-modified carbon microfibers. The carbon microfibers were prepared by carbonizing cotton fibers with a porous structure and a large specific surface area, which showed promising characteristics as an efficient inexpensive HER electrocatalyst<sup>[58]</sup>.

### Freestanding electrocatalyst/electrode

In addition to preparing binder-free electrocatalysts by off-the-shelf substrates, self-supported electrocatalysts could also be directly prepared using the bottom-up approach, namely freestanding electrocatalysts. The freestanding electrocatalyst with the absence of an interface, or denoted as the integrated catalyst electrode, enables a faster electron transfer rate through the interior of the electrodes.

The electrospinning technique is efficient in preparing freestanding electrocatalysts. For instance, Yang *et al.* fabricated novel Ni/NiO-carbon nanotubes (CNTs) composite nanofibers by electrospinning and followed thermal treatment<sup>[59]</sup>. Without extra reducing agents and carbon source, the Ni(Ac)<sub>2</sub>/polyvinylpyrrolidone (PVP) precursor can decompose to reductive gaseous H<sub>2</sub>, CO, CH<sub>4</sub> during the vacuum heat treatment, which could facilitate the NiO reduction and CNT growth. The optimized Ni/NiO-CNTs composite can deliver an excellent HER activity ( $\eta_{10} = 98$  mV) in 1 M KOH<sup>[59]</sup>. The freestanding CNF-Ni/NiO-Pd electrode was also prepared by Barhoum *et al.* via electrospinning, pyrolysis, and atomic layer deposition, sequentially<sup>[60]</sup>. This self-supported composite was employed as a highly efficient HER electrocatalyst. The surface graphitic layers can keep the Ni/NiO from corrosion, and the synergistic effect of different substances at the interfaces attributed the catalyst to excellent performance. The optimized CNF-Ni/NiO-Pd electrocatalyst exhibited a low overpotential ( $\eta_{10} = 63$  mV) and a remarkably small Tafel slope of 72 mV dec<sup>-1</sup><sup>[60]</sup>. As shown in Figure 4A, Li *et al.* prepared the Ni/CeO<sub>2</sub>@N-CNFs catalyst consisting of Ni/CeO<sub>2</sub> hetero-nanoparticles and N-doped carbon nanofibers using the electrospinning-carbonization method<sup>[61]</sup>. The metal/semiconductor heterojunction consisting of Ni/CeO<sub>2</sub> can trigger the self-driven charge transfer and thus facilitate the charge transfer rate, leading to the suitable adsorption energies for reactive intermediate species. Therefore, the Ni/CeO<sub>2</sub>@N-CNFs electrocatalyst showed superb HER activities with an overpotential of 100 mV at 10 mA cm<sup>-2</sup><sup>[61]</sup>. Chemical reduction is another feasible method for obtaining freestanding electrodes. Tao *et al.* first prepared 3D Ni nanofiber material as an electrode through a magnetic-field-assisted reduction method and then modified the 3D Ni electrode by FeCl<sub>3</sub> solution to obtain Fe@Ni-nanofiber electrodes<sup>[62]</sup>. The distinctive structure of 3D electrodes guaranteed full exposure of the catalytic sites and rapid mass and charge transfer. Therefore, this Fe@Ni nanofiber electrode displayed HER excellent activity, with overpotential as low as 55 mV at 10 mA cm<sup>-2</sup><sup>[62]</sup>. In our previous work, we reported a simple procedure for preparing a freestanding surface disordered NiCu solid solution (NiCuDSS) as an efficient HER electrode [Figure 4B-E]. During the hydrothermal reduction process, NH<sub>4</sub><sup>+</sup> tailored the reduction/nucleation rate of Cu<sup>2+</sup>/Ni<sup>2+</sup> ions, leading to its special intertwined 3D microstructure. The unique 3D framework can practically provide a fast electron conduction path and promote bubble separation from the electrode surface. The optimized catalyst displayed superior HER activity (-322 mV at 1,000 mA cm<sup>-2</sup>) and outstanding durability. The theoretical calculations demonstrated that the substitution of Cu can facilitate the hydroxyl desorption from the active sites and thus enhance the kinetics of the overall Volmer reaction<sup>[63]</sup>. Additionally, Li *et al.* synthesized a composite of N/P co-doped carbon shell-coated Ni-Ni<sub>3</sub>P nanoparticles on 3D graphene frameworks via sequential hydrothermal and thermal treatments. As a result, the obtained Ni-Ni<sub>3</sub>P@NPC/rGO electrocatalyst exhibited superior HER electrocatalytic performance<sup>[64]</sup>.

Briefly, the interfacial charge transfer resistance between electrocatalyst and conductive substrate can greatly affect the overall catalytic performance of electrocatalyst. The electron transfer between the conductive substrate and electrocatalyst can be facilitated by chemically *in-situ* growth of active species on a conductive substrate. In addition, the intrinsic conductivity of freestanding electrocatalysts without a conductive substrate needs special attention.

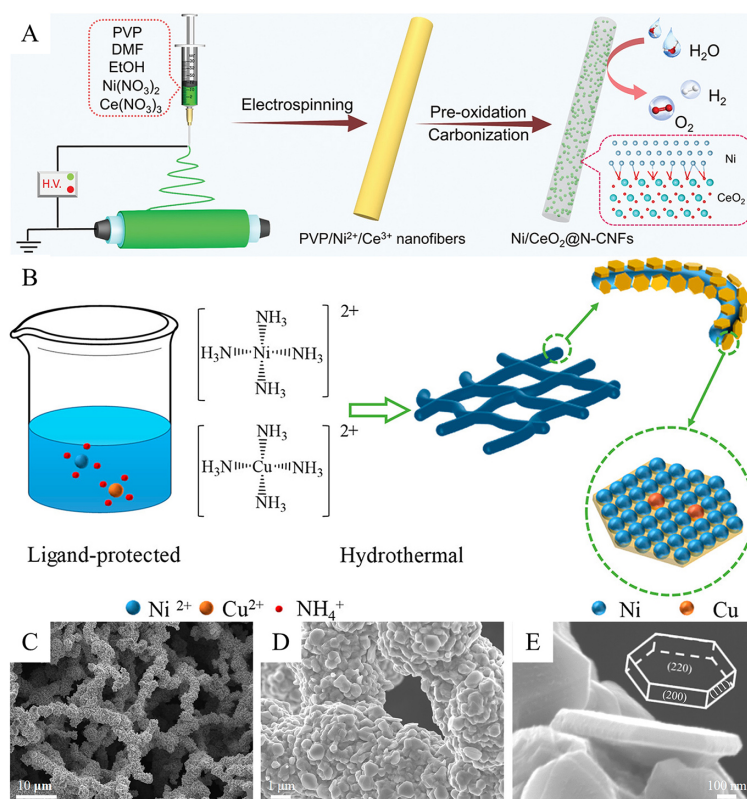


**Figure 4.** (A) Schematic illustration of the synthesis process of Ni/CeO<sub>2</sub>@N-CNFs. (B) Schematic representation of the preparation of NiCuDSS electrocatalysts. (C-E) SEM images of prepared Ni<sub>0.95</sub>Cu<sub>0.05</sub>DSS at different magnifications. This figure is quoted with permission from Li *et al.*<sup>[61]</sup> and Zhang *et al.*<sup>[63]</sup>.

### Internal interface of electrocatalyst

For enhancing the intrinsic catalytic activity of materials, an efficient approach is to create atomic-level or phase-level heterogeneous interfaces inside the electrocatalysts. Multi-interface catalysts in the electrocatalytic field, defined as the catalysts containing interfaces between different components, have received a lot of attention. Interesting physicochemical features could be induced towards the multi-interface catalysts owing to the differences in the geometric and electronic structures of the unequal components. The preferred combination of different components thus can modulate the electrocatalytic reaction pathways and improve reactive kinetics. Although interfaces with variable atomic arrangements can lead to different electron transfer or interfacial resistances, two distinctive interfacial effects have been well identified, namely the ensemble and electron effects. The former originates from the multi-component heterointerfaces, where the interconnected active sites with different local electronic structures can regulate and facilitate the adsorption/desorption procedure of various reactive intermediate species. Therefore, the multi-interface can offer an energetically favorable pathway for a multi-step catalytic process when the individual elementary reaction occurs on its preferred component and so greatly enhances the overall reaction efficiency. Comparatively, the latter (electron effect) means that the different components have electronic interaction at the interface, which could further trigger an interfacial charge redistribution. As a consequence, the adsorption behaviors of key intermediates could be modulated by coupling their electronic structures via electron effect. It may be noted that in a composite electrocatalyst, the ensemble effect and electron effect could hardly be clearly separated; actually, they synergistically accelerate the HER process. Therefore, the rational multi-interface engineering holds great promise to maximize these effects. In order to achieve the atomic design of multi-interfaces, several innovative preparation methods have been

explored, e.g., defecting engineering, vacancy or heteroatom doping, the phase-level heterostructure engineering, *etc.*

#### *Atomic interface via defect engineering*

The defect can be defined as the nonuniform composition in a material, including vacancies, heteroatom dopants, *etc.*, which could significantly affect the electron distribution around the defective sites. The electronic arrangement of the catalyst is closely related to its catalytic activity; consequently, atomic defect engineering could effectively tune the electronic configuration of catalysts, which, in turn, is used to regulate its electrocatalytic performance.

The rational design of non-metallic element vacancies has been revealed as a convenient defect engineering strategy to enhance catalytic activity. For instance, by introducing sulfur vacancies to  $\text{Ni}_3\text{S}_2$ , Jia *et al.* successfully tuned the hydrogen adsorption behaviors on Ni sites to improve HER activity ( $\eta_{10} = 88 \text{ mV}$ ) in 1 M KOH<sup>[65]</sup>. Additionally, oxygen vacancies have also attracted increasing attention. Li *et al.* prepared Ni/Fe/Mo-based electrocatalyst with oxygen vacancies on NF, which was in situ converted to amorphous NiFeMo (oxy)hydroxide during electrocatalysis, exhibiting outstanding intrinsic activity and sufficient active sites for alkaline HER<sup>[66]</sup>. The Ni/MoO<sub>2</sub> has been proven to be highly reactive for hydrogen production. Liang *et al.* synthesized an efficient HER catalyst (Ni/MoO<sub>2-x</sub>) consisting of a Ni nanocluster loaded on the surface of oxygen-vacancy-rich MoO<sub>2</sub><sup>[67]</sup>. X-ray photoelectron spectroscopy (XPS) results indicated that the Ni-O-Mo bonds and oxygen vacancies promoted the migration of electrons from the oxygen to the nickel atom. Furthermore, the theoretical calculations revealed that charge transfer optimized the free energy of intermediates on Ni/MoO<sub>2-x</sub>, which endowed it with excellent catalytic properties<sup>[67]</sup>.

Metal ion doping has also been shown to be another effective approach to modulating the electronic configuration of catalysts. For example, based on Ni/Co-doped MoSe<sub>2</sub> catalysts, Mao *et al.* revealed that doping Ni/Co atoms could effectively modulate the electronic structure of MoSe<sub>2</sub><sup>[68]</sup>. Experimental and theoretical analyses showed that the doped Ni/Co atoms can regulate the position of the *d*-band center and optimize electrical conductivity of catalyst, which, in turn, adjusts the strength of the interactions between adsorbed hydroxyl ( $\text{OH}_{\text{ad}}$ ) and active sites. The optimal hydroxyl adsorption strength would facilitate the Volmer step, thus enhancing the overall alkaline HER kinetics [Figure 5A-E]<sup>[68]</sup>. As shown in Figure 5F, by controlling the reaction conditions, Zhong *et al.* synthesized Ni-doped CoSe with and without Co vacancies, respectively<sup>[69]</sup>. Theoretical and experimental results demonstrated that the Co vacancy and Ni atom located in the vicinity of Se atoms synergistically affect its electron distribution, leading to the upshift of Se 4p(z) orbital. Consequently, the  $\Delta G_{\text{H}}$  of Se atoms was significantly optimized, resulting in an advanced HER activity<sup>[69]</sup>. Jiao *et al.* designed an effective strategy for increasing quantity of active sites by annealing Ni-MOF at different temperatures. The incorporation of trivalent  $\text{Ni}^{3+}$  resulted in a delicate atomic rearrangement and provided more catalytic active sites. Therefore, the as-prepared Ni/NiO nanoparticles displayed excellent HER performance ( $\eta_{10} = 41 \text{ mV}$ )<sup>[70]</sup>. Tang *et al.* prepared a heterostructure catalyst consisting of V-doped NiFe layered double hydroxide (LDH) and Ni nanoparticles, possessing excellent HER catalytic performance ( $\eta_{10} = 19 \text{ mV}$ )<sup>[71]</sup>.

Introducing vacancies or heteroatom dopants into electrocatalysts has been confirmed as useful atomic interface engineering to enhance the electrocatalytic performance. However, some problems still need to be solved. For instance, there remains a need for a greater focus on the stability and *in-situ* reconstruction of defect-rich catalysts. Additionally, the precise control of the coordination environment of the doping site has yet to be available.

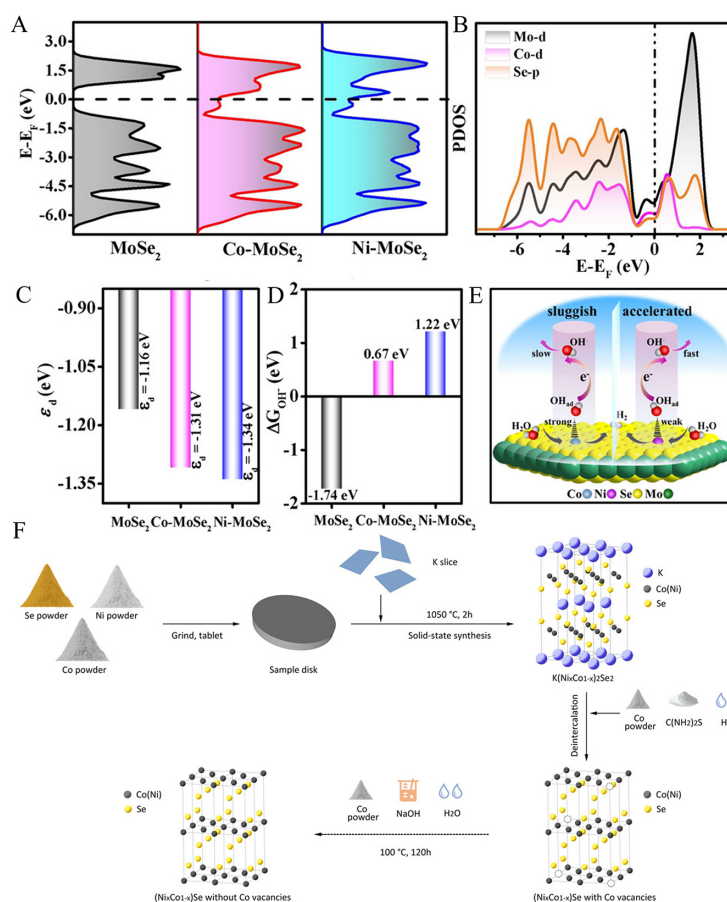


**Figure 5.** (A) The TDOS charts of  $\text{MoSe}_2$ ,  $\text{Co-MoSe}_2$ , and  $\text{Ni-MoSe}_2$ . (B) The PDOS charts of  $\text{Co-MoSe}_2$ . (C) The comparison of d-band centers ( $\epsilon_d$ ) of  $\text{MoSe}_2$ ,  $\text{Co-MoSe}_2$ , and  $\text{Ni-MoSe}_2$ . (D) The Gibbs free energy of  $\text{OH}_{\text{ad}}$ . (E) Schematic diagram of catalytic action of  $\text{OH}_{\text{ad}}$  transfer in alkaline HER process. (F) Schematic diagram of the synthesis method of  $(\text{Co}_{1-x}\text{Ni}_x)_2\text{Se}_2$  with and without vacancies. This figure is quoted with permission from Mao *et al.*<sup>[68]</sup> and Zhong *et al.*<sup>[69]</sup>.

### Interface at heterostructures

The unique physicochemical properties of heterostructured electrocatalysts lead to their excellent HER performance. Heterostructured electrocatalysts composed of different components usually have higher catalytic activity than a single-component catalyst due to the aforementioned synergistic ensemble and electron effects. Therefore, developing heterostructured electrocatalysts with distinctive ensemble effect/electron effect is considered an effectual approach to obtain satisfactory HER performance.

The different multi-components usually have specific catalytic activities for different elementary steps (for distinct intermediates). When these active sites are rationally combined, the overall reaction kinetics thus can be synergistically enhanced. For example, nickel oxide could effectively expedite the water adsorption and dissociation step to generate protons, while metallic nickel can further facilitate hydrogen desorption to generate hydrogen molecules. Based on this dual active site conception, Huang *et al.* developed heterostructured efficient HER catalysts ( $\text{Mo-NiO/Ni}$ ) by doping metal Mo atoms into NiO and coupled with metallic Ni<sup>[72]</sup>. Theoretical and experimental analyses have been used to comprehensively investigate its catalytic mechanisms. Doping Mo heteroatoms into NiO could not only accelerate the water dissociation and rapid transfer of H to the adjacent Ni sites to generate  $\text{H}_2$  but also maintain the structural stability of NiO crystal [Figure 6A-C]. As a consequence, the  $\text{Mo-NiO/Ni}$  catalyst exhibited an excellent HER



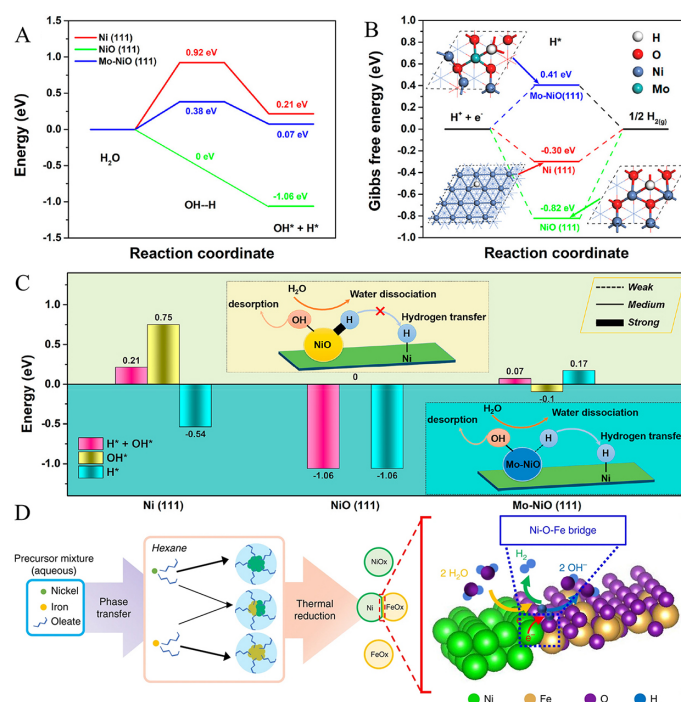


**Figure 6.** (A) Calculated H<sub>2</sub>O dissociation barriers and (B) Gibbs free energies of H adsorption on different theoretical models. (C) Summary of adsorption energy of various reactive intermediates on the Ni-γ-Fe<sub>2</sub>O<sub>3</sub> surfaces. (D) Schematic diagram of the catalyst preparation and the representation of the alkaline HER process on the Ni-γ-Fe<sub>2</sub>O<sub>3</sub> interface. This figure is quoted with permission from Huang *et al.*<sup>[72]</sup> and Suryanto *et al.*<sup>[76]</sup>.

performance with  $\eta_{10}$  of 50 mV and the Tafel slope of 86 mV dec<sup>-1</sup><sup>[72]</sup>. Gu *et al.* synthesized a 3D sponge built via graphene nanocages in which Ni nanoparticles and single atoms coexisted using a facile one-pot strategy<sup>[73]</sup>. The H<sub>2</sub>O molecule was preferentially adsorbed on the atomic Ni sites within the graphene cage, then dissociated into OH<sub>ad</sub> and H<sub>ad</sub>. Subsequently, Ni nanoparticles provided active sites for H adsorption to produce molecular hydrogen. The synergistic catalytic effect between Ni nanoparticles and atomic Ni sites endowed the composite catalyst with excellent HER performance ( $\eta_{10} = 27$  mV)<sup>[73]</sup>. Pt electrodes have excellent catalytic HER performance under acidic conditions, while their HER performance under alkaline conditions is unsatisfactory owing to the lack of water adsorption/dissociation sites. To enhance the HER activity of Pt electrodes in alkaline conditions, Xue *et al.* modified the electrode with Ni-Fe clusters. This heterostructured catalyst exhibited an excellent HER performance, which mostly originated from the synergistic promotion of the facilitated water dissociation ability of Ni-Fe clusters and the optimized hydrogen adsorption ability of Pt<sup>[74]</sup>. Additionally, a special heterostructured HER catalyst (Ni/NiFe-LDO), comprising Ni nanoparticles and NiFe-layered double oxide (LDO) on NF, was successfully constructed, which exhibited  $\eta_{10} = 29$  mV in 1.0 M KOH electrolyte. Detail characterizations indicated that the synergistic interface effect between NiFe-LDO nanosheets and Ni nanoparticles improved its HER activity. The metal oxides were beneficial for water activation because of their strong H<sub>2</sub>O adsorption ability; subsequently, OH was adsorbed on NiO active sites; meanwhile, Ni nanoparticle active sites were responsible for the adsorption of H. In summary, it has been widely acknowledged that properly constructing a multi-component interface could significantly enhance the kinetics of Volmer-step reaction via the distinctive ensemble effect as decoupling the generation and desorption of hydrogen intermediate<sup>[75]</sup>.

In heterogeneous catalysts, interfacial electron transfer could be initiated between different components due to their unequal energy band structures, leading to changes in the adsorption and desorption behavior of

intermediates, which is strongly associated with the HER activity of the electrocatalyst. Therefore, the rational design of efficient alkaline HER electrocatalysts could also be realized by modulating the electronic interactions at the interface. For instance, a nanoparticle catalyst with abundant metallic Ni/ $\gamma$ -Fe<sub>2</sub>O<sub>3</sub> interfaces was developed as an efficient HER electrocatalyst, as shown in Figure 6D. Theoretical calculations indicated that the strong electronic interactions at the Ni/ $\gamma$ -Fe<sub>2</sub>O<sub>3</sub> interfaces resulted in its good HER catalytic activity<sup>[76]</sup>. Sun *et al.* developed a series of hybrid electrocatalysts via implanting bixbyite-type lanthanide metal sesquioxides in metallic Ni toward HER<sup>[77]</sup>. The Yb<sub>2</sub>O<sub>3</sub> could provide abundant active sites and optimize the free energies of water dissociation and hydrogen adsorption. Therefore, the screened Ni/Yb<sub>2</sub>O<sub>3</sub> electrocatalyst exhibited excellent HER performance ( $\eta_{10}$  = 20 mV) and outstanding durability (360 h at 500 mA cm<sup>-2</sup>)<sup>[77]</sup>. The interphasic synergy with charge redistribution in monometallic structures was also reported to successfully tune the adsorption-desorption strength of intermediate species (H/OH) in HER processes. Electronic structure analysis showed that a lot of Ni *d* band electrons at the Fermi level could accelerate the charge transfer from Ni(OH)<sub>2</sub> to Ni-N/Ni-C. Accordingly, the prepared Ni(OH)<sub>2</sub>@Ni-N/Ni-C heterostructured electrocatalyst displayed decent HER activity with an overpotential of 113 mV at 100 mA cm<sup>-2</sup><sup>[78]</sup>. Yang *et al.* obtained a hybrid electrocatalyst via anchoring metallic Ir nanoparticles on Ni-MOF nanosheets<sup>[79]</sup>. The interaction between Ir and Ni-MOF promoted the charge redistribution by the Ni-O-Ir bridge, inducing the adsorption optimization of H<sub>2</sub>O and intermediate species, thus enhancing the electrochemical kinetics of pH-universal HER processes<sup>[79]</sup>. Analogously, it was shown that the charge transfer behaviors at different heterogeneous interfaces between metals and metal oxide-containing components, such as Co-Ni-P/MoS<sub>2</sub><sup>[80]</sup>, Ni/Ni(OH)<sub>2</sub><sup>[81,82]</sup>, Ni/W-Ni(OH)<sub>2</sub><sup>[83]</sup>, Ni/MoO<sub>2</sub><sup>[84]</sup>, Ni/MoN<sup>[85]</sup>, and Ni/NiO-Ti<sub>3</sub>C<sub>2</sub>T<sub>x</sub> MXene<sup>[86]</sup>, could confer superior catalytic performance. In addition, constructing the electrocatalysts with multiple interfaces has been shown to be a feasible scheme for HER electrocatalysts. For example, Zhou *et al.* constructed a Ni-CeF<sub>3</sub>-VN multi-interfaces catalyst and displayed excellent HER activity ( $\eta_{10}$  = 33 mV)<sup>[87]</sup>. The experimental and theoretical analyses showed that electrons moved from Ni to VN/CeF<sub>3</sub>, resulting in the acceleration of Volmer step on Ni/VN interface and recombination of H on Ni/CeF<sub>3</sub> interface, respectively, thus synergistically facilitating the rate of the multi-step HER in alkaline solution<sup>[87]</sup>. Liu *et al.* reported the multi-interface coil-like NiS-Ni<sub>2</sub>P/Ni electrocatalyst prepared on NF. The NiS/Ni and Ni<sub>2</sub>P/Ni interfaces were served as electrochemical active sites and exhibited superior HER catalytic activity with overpotentials of 115 and 53 mV at 10 mA cm<sup>-2</sup> in neutral and alkaline electrolyte<sup>[88]</sup>.

Moreover, metal-organic polymers, particularly conjugated variants, have become increasingly important in the field of electrocatalysis due to their customizable composition, varying metal oxidation states, abundant active sites, and impressive conductivity. These polymers can be prepared under relatively mild conditions. By fine-tuning metal active sites and strategically using functionalized ligands, it is possible to precisely design active sites and foster strong interactions between ligands and metal sites. Therefore, polymers can also be utilized to modify the internal interface of electrocatalyst. For example, Liu *et al.* prepared a self-supported bimetallic Mo-Ni-C<sub>3</sub>N<sub>3</sub>S<sub>3</sub> CP (Mo-NT@NF), featured by robust metal-ligand interactions and varying H<sub>2</sub>O adsorption energy<sup>[89]</sup>. A range of Mo-NT@NF samples were prepared using a simple solvothermal method, and their multivalent metal states and performance towards HER were systematically assessed. The theoretical calculations and experiments revealed that the strong adsorption of the Mo<sup>5+</sup> site of water molecules weakens the O-H bond, in conjunction with efficient proton transfer by the proton relay N and S, leading to a highly effective HER catalysis on the site<sup>[89]</sup>. Zhang *et al.* presented a simple and cost-effective approach to fabricate ultrasmall Ni/NiO<sub>x</sub> heterostructures coated with carbon nano-onions (CNOs) through a single-step thermal decomposition of ultra-thin 2D Ni-based CPs (CPs)<sup>[90]</sup>. The rapid low-temperature graphitization of CPs is crucial for enhancing the performance and scalability of the catalysts prepared. By confining the process within low-temperature graphitization conditions, the ultrasmall size of the Ni/NiO<sub>x</sub> heterojunction (< 5 nm) is guaranteed, leading to a significant increase in interfacial areas and a concurrent rise in active site density. Given the favorable electronic configuration of

Ni<sup>3+</sup> for OH<sub>ad</sub> adsorption, the ultrasmall NiO<sub>x</sub> phase enhances the intrinsic catalytic activity for water decomposition. The low-temperature graphitization process also allows CNOs to maintain abundant hydrophilic functional groups, facilitating efficient mass transfer<sup>[90]</sup>.

For multi-component heterostructured electrocatalysts, decoupling the different elementary steps on various active components has been shown to improve the overall reaction kinetics. Moreover, regulating the charge transfer behavior between diverse components can also reduce the reaction energy barrier or tune intermediate adsorption behaviors, which is an effective strategy to enhance the catalytic performance.

### Electrocatalyst/electrolyte interface

In addition to the intrinsic activity of the electrocatalyst, the mass transport between the electrocatalyst and electrolyte interface is also very important for the overall reaction performance. Especially in the high current density condition, a great many of bubbles would be generated on the electrode surface, which will hinder the contact between the electrolyte and electrode, bringing about a decline in catalytic performance. Through the interfacial wettability engineering of the electrode surface and the rational design of electrical double layer (EDL) structure, the mass/electron transfer between reactive species and active sites can be well promoted to improve the HER performances.

#### Wettability

The wettability of electrocatalysts can significantly affect the catalytic activity under high current density conditions. The most distinctive difference between low (< 100 mA/cm<sup>2</sup>) and high current HER processes is the population of generated gas bubbles during the reaction. If gas bubbles cannot timely detach from the electrode surface, the small air bubbles would coalesce into larger ones as they minimize their surface energy. The large air bubble coverage on electrodes would create an insulator barrier between electrolyte and catalysts, resulting in shrunken effective surface area and high cross-interface ionic resistance with deteriorated HER catalytic performance. Moreover, the attached gas bubbles will continue to grow until the increased buoyancy overcomes the adhesion force between the bubble and catalyst, leading to the induced inner stress at the bubble/catalyst interface which could potentially trigger severe structural damage with compromised catalytic activity. Therefore, engineering the (electrocatalyst/electrolyte) interfacial hydrophilicity and aerophobicity can provide a fast mass and charge transfer pathway to improve the electrocatalytic activity.

Kim *et al.* fabricated a series of morphology-controlled metallic Ni electrocatalysts to systematically investigate the effect of wettability on hydrogen bubble release behaviors [Figure 7A]<sup>[91]</sup>. The wettability (hydrophilicity or aerophobicity) of the catalyst surface is closely related to its porosity. The optimal superaerophobic Ni electrocatalyst exhibited the best HER performance with the highest porosity of approximately 52% among the Ni catalysts. It is observed that the unique superaerophobic surface structure of the metallic Ni electrocatalyst combined with the effective mass transport can accelerate the detachment of H<sub>2</sub> bubbles, substantially improving catalytic performance<sup>[91]</sup>. As shown in Figure 7B-M, Xu *et al.* first prepared 3D-printed Ni electrodes, modified with active materials of MoNi<sub>4</sub> and NiFe LDH, which exhibited superior electrocatalytic HER performance<sup>[92]</sup>. The special porous structure of 3D Ni electrodes allows fast bubble generation and release, providing generous active sites. The MoNi<sub>4</sub>@3D Ni electrode only required an overpotential of 104 mV at 500 mA cm<sup>-2</sup><sup>[92]</sup>. Fujimura *et al.* employed Ni microarray electrodes prepared by photolithography and electrodeposition; the correlation between HER efficiency and surface wettability was explored<sup>[93]</sup>. Furthermore, *in-situ* video surveillance of the electrode surface during the HER process clearly demonstrated that the size of generated air bubbles increased as the wettability of the electrode surface decreased. The larger bubbles will increase the ohmic loss and block the active sites on the

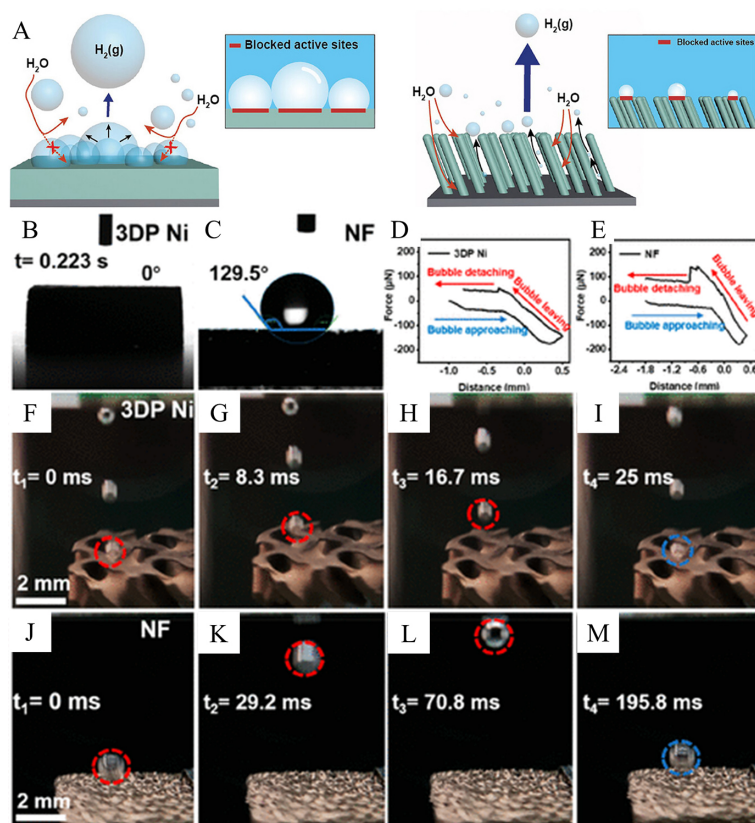


**Figure 7.** (A) Schematic illustrations of the  $\text{H}_2$  bubble-release behavior of different Ni catalysts. (B) Contact angles on 3DP Ni and (C) NF. (D) Bubble adhesive force measurements of 3DP Ni and (E) NF. (F-I) Digital images of bubble release from 3DP Ni and (J-M) NF structures. This figure is quoted with permission from Kim *et al.*<sup>[91]</sup> and Xu *et al.*<sup>[92]</sup>.

electrode surface<sup>[93]</sup>. Shang *et al.* fabricated a HER electrocatalyst (Ni/NiMoN) constructed by NiMoN nanowire arrays modified by metallic Ni nanoparticles on a copper foam<sup>[94]</sup>. Theoretical analysis indicated that the Ni nanoparticles can accelerate  $\text{H}_2\text{O}$  dissociation rate, boosting the feed of protons in the neutral media. Simultaneously, hydrogen bubbles can quickly leave the electrocatalytic surface to refresh the catalytic active sites because the dense nanowire arrays endow the electrode surface with superaerophobic properties. Therefore, the Ni/NiMoN electrode demonstrated excellent HER activity ( $\eta_{10} = 33 \text{ mV}$ ) in a neutral media<sup>[94]</sup>. Li *et al.* designed superhydrophilic Ni-based multi-component array (Ni NCNA) catalyst on NF, which only needed  $-47 \text{ mV}$  to achieve  $10 \text{ mA cm}^{-2}$ . The water contact angle analysis displayed that it took only  $0.2 \text{ s}$  for the water droplet to completely spread on the electrode surface. Owing to its superhydrophilic properties, the Ni NCNA catalyst can operate stably under high current conditions<sup>[95]</sup>. A typical graphite electrode surface can be transformed into a superhydrophilic structure after Ni-Sb alloy modification using a one-step electrodeposition method. Benefiting from its superhydrophilic surface property, the optimized Ni-Sb alloy electrode achieved superior HER electrocatalytic performance<sup>[96]</sup>. Moreover, Yu *et al.* prepared a Ni-Mo-based catalyst with superhydrophilic and aerophilic surfaces. Owing to its high intrinsic activity and porous structure, the Ni-Mo-based catalyst presented remarkable HER activity in all-pH media<sup>[97]</sup>. Therefore, the appropriate modulation of surface wettability, specifically, minimizing the size of gas bubbles at detachment, would be beneficial to alleviate the inner stress and facilitate the rapid release of the generated air bubbles from the electrode surface, enabling enhanced high current density HER performance.



### Electrical double layer

The EDL is where the electrochemical reaction takes place. The inner/outer Helmholtz plane (IHP/OHP) and the diffuse layer together form the EDL [Figure 8]<sup>[98]</sup>. IHP is crucial for an electrochemical reaction, which contains various reaction-involving molecules and ions. For alkaline HER, the main species are H<sub>2</sub>O, adsorbed H<sub>ad</sub> and OH<sub>ad</sub>/OH<sup>-</sup> from water dissociation, and H<sub>2</sub> and specific cations from the electrolyte solution. The transfer impedance of reactive species in EDL can increase the overall reaction overpotential and energy loss. Unfortunately, it is very hard to directly monitor the interfacial effect of EDL during alkaline HER due to the lack of effective methods for detecting interfacial species. This is because the structural or compositional changes of EDL could only be studied via *in situ/operando* technology due to its instantaneous property changes with the applied electric field, and the thickness of EDL is only around 1-10 nm. Despite the difficulties in studying EDL, researchers have been working to reveal the *in-situ* changes in EDL during the HER process to direct the rational design of excellent HER electrocatalysts.

For example, Zhang *et al.* employed interfacial chemistry engineering to tune the adsorption free energy of H<sub>2</sub>O dissociation and H simultaneously<sup>[99]</sup>. The hybrid Ni<sub>0.2</sub>Mo<sub>0.8</sub>N microrod arrays supported on NF were decorated with Ni nanoparticles. Theoretical analysis suggested that the Ni<sub>0.2</sub>Mo<sub>0.8</sub>N and Ni acted as adsorption active sites for hydrogen and hydroxyl, respectively, synergistically promoting alkaline HER. The resulting Ni<sub>0.2</sub>Mo<sub>0.8</sub>N/Ni electrocatalyst exhibited excellent HER electrocatalytic activity (-70 mV at 300 mA cm<sup>-2</sup>). Moreover, further finite-element-based simulations indicated that an enhanced local electric field around Ni particles was formed, which led to an increased hydrated K<sup>+</sup> concentration in IHP and thus accelerated the subsequent water dissociation elementary step [Figure 9A]<sup>[99]</sup>. Similarly, Gao *et al.* reported a nanocone-assembled Ru<sub>3</sub>Ni electrocatalyst, which displayed a superior HER electrocatalytic performance with an overpotential of 168 mV at 1,000 mA cm<sup>-2</sup> and a high mass activity with a low loading of only 0.08 mg cm<sup>-2</sup> of Ru<sub>3</sub>Ni<sup>[100]</sup>. The density functional theory (DFT), finite-element-based simulations and experimental results comprehensively revealed that the enrichment of hydrated K<sup>+</sup> at the sharp tip led to the intensive polarization of interfacial H<sub>2</sub>O and reduced the energy barrier for water dissociation [Figure 9B]<sup>[100]</sup>. Tuning the local reaction environment in alkaline electrolyte has been shown to be a potential method to improve the HER catalytic performance. Tan *et al.* successfully developed a local H<sub>3</sub>O<sup>+</sup>-rich microenvironment, namely a local acid-like environment, in 1 M KOH solution and achieved superior HER performance<sup>[101]</sup>. Comprehensive analyses indicated that the formation of localized acid environments was mainly due to the following reasons: oxygen vacancy-rich MgO nanosheets can promote the production of H<sub>3</sub>O<sup>+</sup>; the redistribution of electrons between Pt and MgO results in the formation of electron-rich Pt species; owing to the electrostatic attraction, H<sub>3</sub>O<sup>+</sup> accumulates around negatively charged Pt species. Consequently, as shown in Figure 9C-E, the Pt/MgO electrocatalyst displayed superb intrinsic HER activity ( $\eta_{10} = 39$  mV) in 1 M KOH, which is even comparable to Pt/C under acidic conditions<sup>[101]</sup>.

The additive in electrolyte can also regulate the structure of EDL to improve HER reaction kinetics. For instance, Amaral *et al.* investigated the impact of incorporating three homemade salicylate ([Sal])-based ionic liquids (ILs) in KOH electrolyte solutions on HER<sup>[102]</sup>. Electrochemical analysis indicated increased currents and a slight impact on activation energy in the IL-containing electrolytes. Tafel analysis and EIS demonstrate that the Volmer reaction is the rate-limiting step of HER, with a significant reduction in overall impedance observed in the IL-enhanced electrolytes, promoting stable operation. The charge transfer and polarization resistances are notably lowered in the IL-containing solutions, particularly following the addition of [Bmim][Sal], with the influence of the additives diminishing as temperature rises. This research suggested that incorporating small quantities of specific ILs into KOH electrolytes could enhance HER performance in alkaline environments<sup>[102]</sup>. Then, Amaral *et al.* also synthesized two bromide-based ILs and studied their impact as additives in alkaline electrolytes for HER<sup>[103]</sup>. Electrochemical analysis was conducted



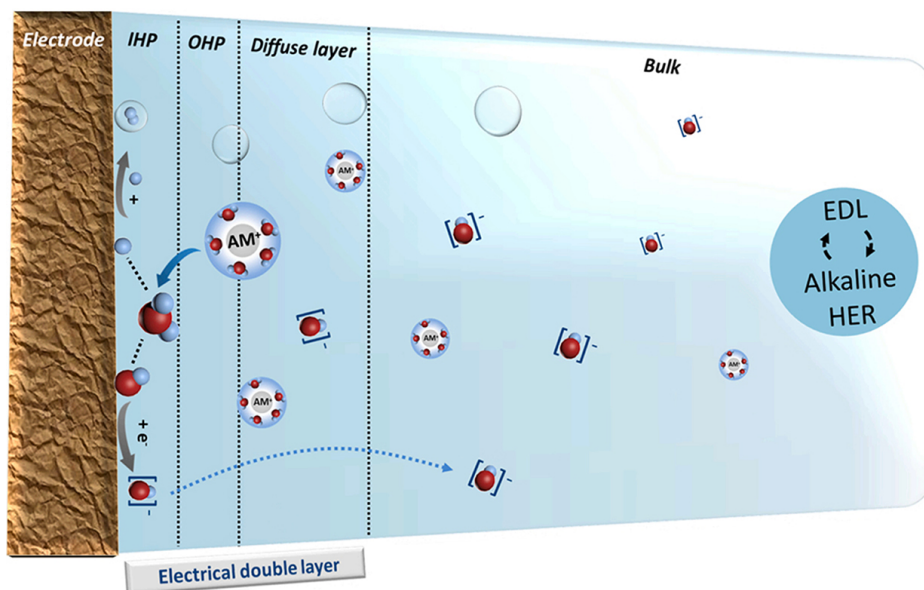


**Figure 8.** Simplistic view of EDL for alkaline HER. Red: O; Blue: H. This figure is quoted with permission from Jiang *et al.* [98].

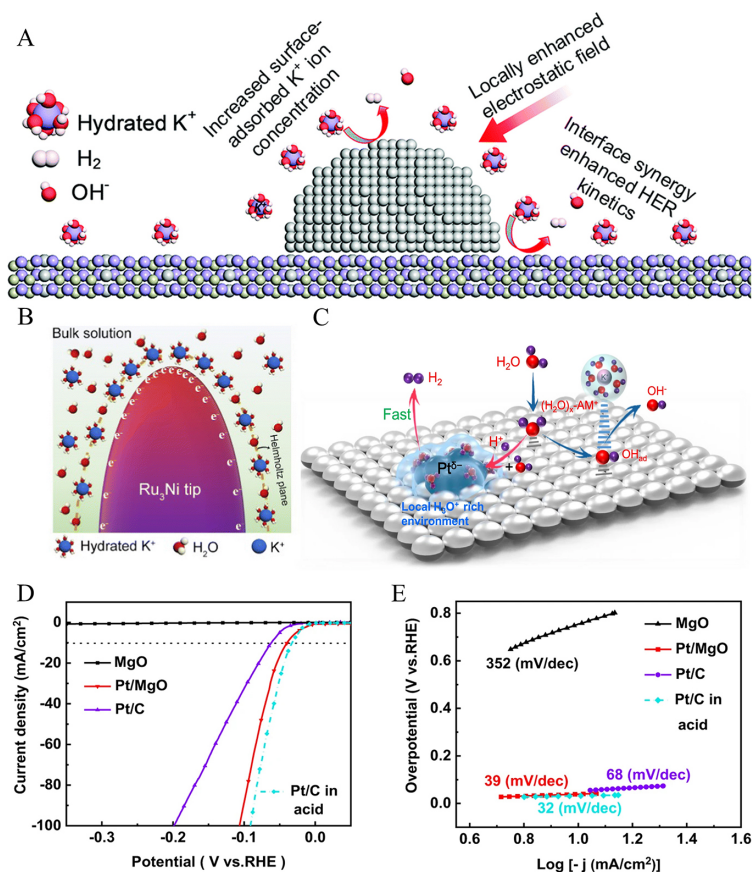


**Figure 9.** (A) Schematic diagram of the excellent activity of  $\text{Ni}_{0.2}\text{Mo}_{0.8}\text{N}/\text{Ni}$ . (B) Schematic representation of the interfacial model for  $\text{Ru}_3\text{Ni}$ . (C) Schematic representation of reaction mechanism. (D) Linear sweep voltammetry (LSV) curves of  $\text{MgO}$ ,  $\text{Pt}/\text{MgO}$ , and  $\text{Pt}/\text{C}$ . (E) The corresponding Tafel plots were calculated from the LSV curves of  $\text{MgO}$ ,  $\text{Pt}/\text{MgO}$ , and  $\text{Pt}/\text{C}$ . This figure is quoted with permission from Zhang *et al.* [99], Gao *et al.* [100] and Tan *et al.* [101].

using Pt electrodes in an 8 M KOH electrolyte without ILs and with the addition of 1 or 2 vol.% of each IL. The inclusion of 2 vol.% of [Beim][Br] resulted in higher current densities. These homemade bromide-based additives influenced the HER kinetics, resulting in slightly elevated Tafel slopes and minor changes in the charge transfer coefficient and exchange current density. Impedance measurements revealed a significant reduction in overall impedance in the presence of the bromide-based ILs in the alkaline electrolytes, with Nyquist plots showing a predominant intermediate frequency relaxation associated with adsorbed hydrogen. The bromide-based ILs demonstrate an improvement in electrolyte properties and enhance the efficiency of alkaline electrolysis<sup>[103]</sup>.

## SUMMARY AND OUTLOOK

In conclusion, as HER is an electrochemical process involving a ternary gas-liquid-solid interface, the rational design of multi-interface in electrodes is extremely significant for enhancing alkaline HER performance. Herein, we summarized the recent progress in interface engineering for Ni-based HER electrocatalysts, including substrate/electrocatalyst interface, internal heterointerface of electrocatalyst, and electrocatalyst/electrolyte interface. The latest advancements of interface engineering on Ni-based catalysts discussed in the review have been summarized in Table 1. The polymer binders can retard the electron transfer across the substrate/electrocatalytic interface (from the conductive substrate to the active site), so the method of in situ grown catalytic active materials on conductive substrates or directly preparing freestanding electrodes has been proposed to solve this problem. The intrinsic catalytic activity of electrocatalyst is closely related to its electronic structure, which can be rationally tuned by engineering its internal heterointerface. For example, the electron distribution at the interface can be well regulated by introducing defects or heterostructures, thus optimizing the adsorption and desorption behavior of key intermediate species to improve the catalytic performance. Moreover, the mass transfer at an electrocatalyst/electrolyte interface is particularly important under high current conditions in HER process. By adjusting the wettability of the catalyst surface and the EDL structure, the mass transport efficiency can be greatly improved. Although great progress and achievements have been made in advanced HER electrocatalysts by multi-interface engineering, several key issues remain to be addressed.

(1) The interfacial compatibility between the conductive substrate and catalytic materials can largely determine their binding strength, thus proving crucial for the overall stability of the electrode, especially for the high current density working conditions in alkaline medium. The generation, coalescence, and detachment of large amounts of gas bubbles could induce great stretch pressure at the interface, which would not only result in decreased effective surface area and high ionic diffusion resistance but also bring fatal damage to the electrode structures. Therefore, delicate interface construction aiming to minimize the bubble size while maximizing their transport/release should be given more attention, which has not been fully investigated.

(2) It is well established that defects or heterogeneous interfaces can lead to charge redistribution at the interface, which can achieve rational regulation of the adsorption/desorption characteristics of key reaction intermediates. As an important intrinsic determinant, the intrinsic electronic structure and interactions with intermediates can also determine the electrocatalyst by influencing the intrinsic conductivity and reaction energy barrier. For alkaline water splitting,  $\text{OH}_{\text{ad}}$  has an important role in both cathodic (HER) and anodic (OER) reactions. It had been pointed out that the adsorption behavior of  $\text{OH}_{\text{ad}}$  is deeply intertwined with OER activity, which is associated with the bonding strength of the active site and oxygen. The crystal field theory provides theoretical guidance for the design of OER electrocatalyst. In octahedral symmetry, the  $d$ -orbital and ligand electrons repel each other, causing the  $d$ -orbital energy levels to split into high-energy orbitals  $e_g$  and low-energy orbitals  $t_{2g}$ . The occupancy of  $e_g$  orbitals in the design of OER catalysts has been

**Table 1. Summary of Ni-based catalysts for alkaline hydrogen evolution reaction**

Catalysts	Substrate	Electrolyte	Current density (mA cm <sup>-2</sup> )	Overpotential (mV)	Ref.
MoO <sub>2</sub> -Ni NWs	Ni foam	1 M KOH	10	58.4	[42]
Ni <sub>4</sub> Co <sub>1</sub> Fe <sub>4</sub> -P	Ni foam	1 M KOH	20	61	[43]
Ni-Cu-P@Ni-Cu	Ni foam	1 M KOH	10	70	[44]
Ru@Ni-MOF	Ni foam	1 M KOH	10	22	[45]
Ni NTAs/NF	Ni foam	1 M KOH	10	101	[46]
MoO <sub>2</sub> /Ni@NF	Ni foam	1 M KOH	10	50.5	[47]
Ni-WO <sub>x</sub> @NF	Ni foam	1 M KOH	10	45.7	[48]
W-NT@NF	Ni foam	1 M KOH	10	88	[49]
Ni/TiO <sub>2</sub>	Ni foam	1 M KOH	10	46	[50]
NiFeCoS <sub>x</sub> @FeNi <sub>3</sub>	FeNi <sub>3</sub> foam	1 M KOH	10	88	[51]
Ni-Co alloy		1 M KOH	10	54	[52]
Cu <sub>2</sub> S@Ni	Cu foam	1M NaOH	500	200	[53]
W <sub>2</sub> C-Ni/CC	Carbon cloth	1 M KOH	10	37	[54]
NiO/Ni@CC	Carbon cloth	1 M KOH	10	40	[55]
Ni-Ni <sub>3</sub> C/CC	Carbon cloth	1 M KOH	10	98	[56]
Ni/V <sub>2</sub> O <sub>3</sub>	Carbon cloth	1 M KOH	10	44	[57]
Ni/NiO-CNTs		1 M KOH	10	98	[59]
C-20Ni-Pd		1 M KOH	10	590	[60]
Ni/CeO <sub>2</sub> @N-CNFs		1 M KOH	10	100	[61]
Fe@Ni NFs		1 M KOH	10	55	[62]
Ni <sub>0.95</sub> Cu <sub>0.05</sub> DSS		1 M KOH	100	179	[63]
Ni-Ni <sub>3</sub> P@NPC/rGO		1 M KOH	20	200	[64]
Vs-Ni <sub>3</sub> S <sub>2</sub> /NF	Ni foam	1 M KOH	10	88	[65]
Ni/NiFeMoO <sub>x</sub> /NF	Ni foam	1 M KOH	10	22	[66]
Ni/MoO <sub>2-x</sub> /NF	Ni foam	1 M KOH	10	27	[67]
Ni-MoSe <sub>2</sub>	Carbon cloth	0.1 M KOH	10	98	[68]
Co <sub>0.9</sub> Ni <sub>0.1</sub> Se		1 M KOH	10	185.7	[69]
Ni/NiO-400	Carbon cloth	1 M KOH	10	41	[70]
P-V-NiFe LDH NSA	Ni foam	1 M KOH	10	19	[71]
Mo-NiO/Ni		1 M KOH	10	50	[72]
SGNCs		1 M KOH	10	27	[73]
NiFe@Pt		0.1 M KOH	10	70	[74]
Ni/NiFe-LDO	Ni foam	1 M KOH	10	29	[75]
Ni-Fe NP	Carbon fiber paper	1 M KOH	10	46	[76]
Ni/Yb <sub>2</sub> O <sub>3</sub>		1 M KOH	10	81	[77]
Ni(OH) <sub>2</sub> @Ni-N/Ni-C	Ni foam	1 M KOH	10	60	[78]
Ir@Ni-NDC		1 M KOH	10	19	[79]
Co-Ni-P/MoS <sub>2</sub>		1 M KOH	10	116	[80]
Ni/Ni(OH) <sub>2</sub>		1 M KOH	10	77	[81]
Ni-Ni(OH) <sub>2</sub> /NF	Ni foam	1 M KOH	10	72	[82]
Cu <sub>2</sub> O@NWNH	Cu foam	1M PBS	10	39	[83]
Ni/MoO <sub>2</sub> @NF-E	Ni foam	1 M KOH	10	19	[84]
Ni-MoN	Cu foam	1 M KOH	100	61	[85]
Ni-NiO/Ti <sub>3</sub> C <sub>2</sub> T <sub>x</sub>		1 M KOH	10	72	[86]
Ni-CeF <sub>3</sub> -VN	Ni foam	1 M KOH	10	33	[87]
NiS-Ni <sub>2</sub> P/Ni/NF	Ni foam	1 M KOH	10	53	[88]
Ni-80	Ni film	1 M KOH	10	135	[91]
MoNi <sub>4</sub> -MoO <sub>2</sub>	3DP Ni	1 M KOH	500	104	[92]

Ni microdots	Cu film	1 M KOH	50	476	[93]
Ni NCNAs	Ni foam	1 M KOH	10	47	[95]
Ni-Sb alloy	Graphite	1 M KOH	10	158	[96]
Pt/Ni-Mo-N-O	Ni foam	1 M KOH	100	40.6	[97]
Ni <sub>0.2</sub> Mo <sub>0.8</sub> N/Ni	Ni foam	1 M KOH	100	40	[99]
NA-Ru <sub>3</sub> Ni/C		1 M KOH	1000	168	[100]

widely used as a descriptor of bonding strength between the active site and oxygen. Transition metal ions with  $e_g$  orbital occupancy approaching 1 generally have better OER intrinsic activity. Active atoms with high occupancy ( $e_g > 1$ ) will be too weakly bonded to oxygen, while low occupancy ( $e_g < 1$ ) will be too strongly bonded to oxygen. Based on the above understanding, for the design of internal heterointerface of electrocatalyst towards alkaline HER, the adsorption strength of  $\text{OH}_{\text{ad}}$  can also be tuned by adjusting the  $e_g$  orbital occupancy of the active site so as to promote water dissociation or alleviate the poison effect of  $\text{OH}_{\text{ad}}$ . Moreover, understanding its intrinsic mechanism is mostly based on the oversimplified theoretical calculations and lack of effective *in-situ* characterization. Therefore, the effect of the internal heterointerface of electrocatalyst is worthy of further study.

(3) At present, few researches focus on mass transfer at gas-liquid-solid interface, namely, electrocatalyst/electrolyte interface. In fact, for the industrial water electrolyzer, the mass transfer capacity of the electrocatalyst under high current conditions is particularly important, which can be improved by engineering wettability and EDL of the electrocatalyst. Nevertheless, the reaction mechanism and its physical structure at the electrocatalyst/electrolyte interface need more in-depth study, which depends on more accurate in situ characterization techniques.

In fact, when optimizing the substrate/electrocatalyst interface, constraints imposed by the substrate characteristics often limit the use of milder methods for in situ growth of active species on the conductive surface. To enhance the intrinsic activity of electrocatalysts, commonly employed methods, such as high-temperature treatments or mechanical ball milling, are utilized to introduce defect sites at the internal interface of electrocatalysts. However, this approach is in conflict with the mild reaction conditions required for optimizing the catalyst-substrate interface, posing challenges to achieving both objectives simultaneously. Furthermore, optimizing the electrocatalyst/electrolyte interface through control of wettability or EDL is predominantly achieved by modulating the surface morphology of the electrocatalyst. However, this process necessitates changes in reaction conditions, making it challenging to simultaneously meet the growth requirements of active species and precisely introduce defect sites, thereby imposing higher demands on material synthesis methods.

Although optimizing three interfaces simultaneously poses certain challenges through conventional experimental methods, the integration of advanced material synthesis techniques can partially mitigate this issue. For example, after growing active species on a conductive substrate using conventional hydrothermal synthesis, plasma etching can introduce vacancy-like defect sites on the electrocatalyst surface. Additionally, techniques such as magnetron sputtering or atomic layer deposition can be combined to precisely fabricate heterostructures on the electrocatalyst surface to enhance the intrinsic catalytic activity. These methods differ from conventional approaches in their ability to circumvent the need for harsh reaction conditions and stringent substrate requirements, thereby enabling simultaneous optimization of all three interfaces alongside traditional preparation techniques.

In summary, the multi-interface design for the electrocatalyst is crucial to the HER electrocatalyst performance, including activity and stability. When designing efficient HER electrocatalysts, it is imperative to consider the synergistical modulation of these three key interfaces simultaneously.

## DECLARATIONS

### Authors' contributions

Proposed the topic of this review: Wang C

Wrote the manuscript: Zhang X, Guo Y, Wang C

Reviewed the manuscript: Wang C

### Availability of data and materials

Not applicable.

### Financial support and sponsorship

This research was supported by the Natural Science Foundation of Shanxi Province (202103021224440), Shanxi Scholarship Council of China and Youth Innovation Promotion Association CAS (2020180).

### Conflicts of interest

All authors declared that there are no conflicts of interest.

### Ethical approval and consent to participate

Not applicable.

### Consent for publication

Not applicable.

### Copyright

© The Author(s) 2024.

## REFERENCES

1. He Q, Zhou Y, Shou H, et al. Synergic reaction kinetics over adjacent ruthenium sites for superb hydrogen generation in alkaline media. *Adv Mater* 2022;34:e2110604. DOI
2. Fan K, Tsang YH, Huang H. Theoretical evidence of self-intercalated 2D materials for battery and electrocatalytic applications. *Energy Mater* 2023;3:300047. DOI
3. Tian X, Li X, Yang T, et al. Porous worm-like NiMoO<sub>4</sub> coaxially decorated electrospun carbon nanofiber as binder-free electrodes for high performance supercapacitors and lithium-ion batteries. *Appl Surf Sci* 2018;434:49-56. DOI
4. Cao X, Zhang L, Huang K, Zhang B, Wu J, Huang Y. Strained carbon steel as a highly efficient catalyst for seawater electrolysis. *Energy Mater* 2022;2:200010. DOI
5. Tian X, Yang T, Song Y, et al. Symmetric supercapacitor operating at 1.5 V with combination of nanosheet-based NiMoO<sub>4</sub> microspheres and redox additive electrolyte. *J Energy Stor* 2022;47:103960. DOI
6. Xu HG, Zhang XY, Ding Y, et al. Rational design of hydrogen evolution reaction electrocatalysts for commercial alkaline water electrolysis. *Small Struct* 2023;4:2200404. DOI
7. Zhu B, Zou R, Xu Q. Metal-organic framework based catalysts for hydrogen evolution. *Adv Energy Mater* 2018;8:1801193. DOI
8. Yan D, Mebrahtu C, Wang S, Palkovits R. Innovative electrochemical strategies for hydrogen production: from electricity input to electricity output. *Angew Chem Int Ed* 2023;62:e202214333. DOI PubMed
9. Li J, Xia Z, Xue Q, et al. Insights into the interfacial lewis acid-base pairs in CeO<sub>2</sub>-loaded CoS<sub>2</sub> electrocatalysts for alkaline hydrogen evolution. *Small* 2021;17:e2103018. DOI
10. Chen Z, Gong W, Wang J, et al. Metallic W/VO<sub>2</sub> solid-acid catalyst boosts hydrogen evolution reaction in alkaline electrolyte. *Nat Commun* 2023;14:5363. DOI PubMed PMC
11. Jin J, Yin J, Liu H, et al. Atomic sulfur filling oxygen vacancies optimizes H absorption and boosts the hydrogen evolution reaction in alkaline media. *Angew Chem Int Ed* 2021;60:14117-23. DOI
12. Liu Y, Feng Q, Liu W, et al. Boosting interfacial charge transfer for alkaline hydrogen evolution via rational interior Se modification.



- Nano Energy* 2021;81:105641. DOI
13. Zhang JZ, Zhang Z, Zhang HB, et al. Prussian-blue-analogue-derived ultrathin Co<sub>2</sub>P-Fe<sub>2</sub>P nanosheets for universal-pH overall water splitting. *Nano Lett* 2023;23:8331-8. DOI
  14. Li Y, Xu T, Huang Q, et al. C<sub>60</sub> fullerene to stabilize and activate Ru nanoparticles for highly efficient hydrogen evolution reaction in alkaline media. *ACS Catal* 2023;13:7597-605. DOI
  15. Zhao X, Li X, Xiao D, et al. Isolated Pd atom anchoring endows cobalt diselenides with regulated water-reduction kinetics for alkaline hydrogen evolution. *Appl Catal B Environ* 2021;295:120280. DOI
  16. Wu J, Fan J, Zhao X, et al. Atomically dispersed MoO<sub>x</sub> on rhodium metallene boosts electrocatalyzed alkaline hydrogen evolution. *Angew Chem Int Ed* 2022;61:e202207512. DOI
  17. Men YN, Tan Y, Li P, et al. Tailoring the 3D-orbital electron filling degree of metal center to boost alkaline hydrogen evolution electrocatalysis. *Appl Catal B Environ* 2021;284:119718. DOI
  18. Jiang Y, Leng J, Zhang S, et al. Modulating water splitting kinetics via charge transfer and interfacial hydrogen spillover effect for robust hydrogen evolution catalysis in alkaline media. *Adv Sci* 2023;10:e2302358. DOI PubMed PMC
  19. Yang W, Li M, Zhang B, et al. Interfacial microenvironment modulation boosts efficient hydrogen evolution reaction in neutral and alkaline. *Adv Funct Mater* 2023;33:2304852. DOI
  20. Wan C, Zhang Z, Dong J, et al. Amorphous nickel hydroxide shell tailors local chemical environment on platinum surface for alkaline hydrogen evolution reaction. *Nat Mater* 2023;22:1022-9. DOI
  21. Zhang R, Li Y, Zhou X, et al. Single-atomic platinum on fullerene C<sub>60</sub> surfaces for accelerated alkaline hydrogen evolution. *Nat Commun* 2023;14:2460. DOI PubMed PMC
  22. Alsabban MM, Eswaran MK, Peramaiah K, et al. Unusual activity of rationally designed cobalt phosphide/oxide heterostructure composite for hydrogen production in alkaline medium. *ACS Nano* 2022;16:3906-16. DOI PubMed PMC
  23. Yi L, Ji Y, Shao P, et al. Scalable synthesis of tungsten disulfide nanosheets for alkali-acid electrocatalytic sulfion recycling and H<sub>2</sub> generation. *Angew Chem Int Ed* 2021;60:21550-7. DOI
  24. Wang X, Long G, Liu B, et al. Rationally modulating the functions of Ni<sub>3</sub>Sn<sub>2</sub>-NiSnO<sub>x</sub> nanocomposite electrocatalysts towards enhanced hydrogen evolution reaction. *Angew Chem Int Ed* 2023;62:e202301562. DOI
  25. Li Z, Yu C, Wen Y, et al. Mesoporous hollow Cu-Ni alloy nanocage from core-shell Cu@Ni nanocube for efficient hydrogen evolution reaction. *ACS Catal* 2019;9:5084-95. DOI
  26. Song J, Jin YQ, Zhang L, et al. Phase-separated Mo-Ni alloy for hydrogen oxidation and evolution reactions with high activity and enhanced stability. *Adv Energy Mater* 2021;11:2003511. DOI
  27. Wang M, Yang H, Shi J, et al. Alloying nickel with molybdenum significantly accelerates alkaline hydrogen electrocatalysis. *Angew Chem Int Ed* 2021;60:5771-7. DOI
  28. Lu W, Li X, Wei F, et al. In-situ transformed Ni, S-codoped CoO from amorphous Co-Ni sulfide as an efficient electrocatalyst for hydrogen evolution in alkaline media. *ACS Sustain Chem Eng* 2019;7:12501-9. DOI
  29. Xu H, Fei B, Cai G, et al. Boronization-induced ultrathin 2D nanosheets with abundant crystalline - amorphous phase boundary supported on nickel foam toward efficient water splitting. *Adv Energy Mater* 2020;10:1902714. DOI
  30. Chen N, Du Y, Zhang G, Lu W, Cao F. Amorphous nickel sulfoselenide for efficient electrochemical urea-assisted hydrogen production in alkaline media. *Nano Energy* 2021;81:105605. DOI
  31. Su J, Wang Q, Fang M, et al. Metastable hexagonal-phase nickel with ultralow Pt content for an efficient alkaline/seawater hydrogen evolution reaction. *ACS Appl Mater Interfaces* 2023;15:51160-9. DOI
  32. Pang QQ, Bai X, Du X, Zhang S, Liu ZY, Yue XZ. Facet modulation of nickel-ruthenium nanocrystals for efficient electrocatalytic hydrogen evolution. *J Colloid Interface Sci* 2023;633:275-83. DOI PubMed
  33. Nguyen DN, Phu TKC, Kim J, et al. Interfacial strain-modulated nanospherical Ni<sub>2</sub>P by heteronuclei-mediated growth on Ti<sub>3</sub>C<sub>2</sub>T<sub>x</sub> MXene for efficient hydrogen evolution. *Small* 2022;18:e2204797. DOI
  34. Li Y, Min K, Han B, Lee LYS. Ni nanoparticles on active (001) facet-exposed rutile TiO<sub>2</sub> nanopyramid arrays for efficient hydrogen evolution. *Appl Catal B Environ* 2021;282:119548. DOI
  35. Su H, Tang Y, Shen H, et al. Insights into antiperovskite Ni<sub>3</sub>In<sub>1-x</sub>Cu<sub>x</sub>N multi-crystalline nanoplates and bulk cubic particles as efficient electrocatalysts on hydrogen evolution reaction. *Small* 2022;18:e2105906. DOI
  36. Liu J, Wang J, Fo Y, et al. Engineering of unique Ni-Ru nano-twins for highly active and robust bifunctional hydrogen oxidation and hydrogen evolution electrocatalysis. *Chem Eng J* 2023;454:139959. DOI
  37. Lu J, Chen S, Zhuo Y, Mao X, Liu D, Wang Z. Greatly boosting seawater hydrogen evolution by surface amorphization and morphology engineering on MoO<sub>2</sub>/Ni<sub>3</sub>(PO<sub>4</sub>)<sub>2</sub>. *Adv Funct Mater* 2023;33:2308191. DOI
  38. Lyu C, Cao C, Cheng J, et al. Interfacial electronic structure modulation of Ni<sub>2</sub>P/Ni<sub>5</sub>P<sub>4</sub> heterostructure nanosheets for enhanced pH-universal hydrogen evolution reaction performance. *Chem Eng J* 2023;464:142538. DOI
  39. Xu Q, Zhang J, Zhang H, et al. Atomic heterointerface engineering overcomes the activity limitation of electrocatalysts and promises highly-efficient alkaline water splitting. *Energy Environ Sci* 2021;14:5228-59. DOI
  40. Wei J, Zhou M, Long A, et al. Heterostructured electrocatalysts for hydrogen evolution reaction under alkaline conditions. *Nanomicro Lett* 2018;10:75. DOI PubMed PMC
  41. Huang C, Zhou J, Duan D, et al. Roles of heteroatoms in electrocatalysts for alkaline water splitting: a review focusing on the reaction mechanism. *Chin J Catal* 2022;43:2091-110. DOI

42. Liu X, Ni K, Niu C, et al. Upraising the O 2p orbital by integrating Ni with MoO<sub>2</sub> for accelerating hydrogen evolution kinetics. *ACS Catal* 2019;9:2275-85. DOI
43. Chang J, Wang W, Wu D, et al. Self-supported amorphous phosphide catalytic electrodes for electrochemical hydrogen production coupling with methanol upgrading. *J Colloid Interface Sci* 2023;648:259-69. DOI
44. Darband GB, Lotfi N, Aliabadi A, Hyun S, Shanmugam S. Hydrazine-assisted electrochemical hydrogen production by efficient and self-supported electrodeposited Ni-Cu-P@Ni-Cu nano-micro dendrite catalyst. *Electrochim Acta* 2021;382:138335. DOI
45. Deng L, Hu F, Ma M, et al. Electronic modulation caused by interfacial Ni-O-M (M= Ru, Ir, Pd) bonding for accelerating hydrogen evolution kinetics. *Angew Chem Int Ed* 2021;60:22276-82. DOI
46. Li D, Hao G, Guo W, Liu G, Li J, Zhao Q. Highly efficient Ni nanotube arrays and Ni nanotube arrays coupled with NiFe layered-double-hydroxide electrocatalysts for overall water splitting. *J Power Sources* 2020;448:227434. DOI
47. Liang W, Dong P, Le Z, et al. Electron density modulation of MoO<sub>2</sub>/Ni to produce superior hydrogen evolution and oxidation activities. *ACS Appl Mater Interfaces* 2021;13:39470-9. DOI
48. Liang W, Zhou M, Lin X, et al. Nickel-doped tungsten oxide promotes stable and efficient hydrogen evolution in seawater. *Appl Catal B Environ* 2023;325:122397. DOI
49. Liu M, Zou W, Qiu S, Su N, Cong J, Hou L. Active site tailoring of Ni-based coordination polymers for high-efficiency dual-functional HER and UOR catalysis. *Adv Funct Mater* 2024;34:2310155. DOI
50. Zhou P, Wang S, Zhai G, et al. Host dependent electrocatalytic hydrogen evolution of Ni/TiO<sub>2</sub> composites. *J Mater Chem A* 2021;9:6325-34. DOI
51. Shen J, Li Q, Zhang W, et al. Spherical Co<sub>3</sub>S<sub>4</sub> grown directly on Ni-Fe sulfides as a porous nanoplate array on FeNi<sub>3</sub> foam: a highly efficient and durable bifunctional catalyst for overall water splitting. *J Mater Chem A* 2022;10:5442-51. DOI
52. Wang J, Shao H, Ren S, Hu A, Li M. Fabrication of porous Ni-Co catalytic electrode with high performance in hydrogen evolution reaction. *Appl Surf Sci* 2021;539:148045. DOI
53. Zhang B, Xu W, Liu S, et al. Enhanced interface interaction in Cu<sub>2</sub>S@Ni core-shell nanorod arrays as hydrogen evolution reaction electrode for alkaline seawater electrolysis. *J Power Sources* 2021;506:230235. DOI
54. Yang B, Fu HC, Chen XH, et al. Nanoarchitectonics for synergistic action coupling of Ni nanoparticles with W<sub>2</sub>C nanowires for highly efficient alkaline hydrogen production. *Appl Surf Sci* 2023;630:157460. DOI
55. Chen H, Ge D, Chen J, et al. In situ surface reconstruction synthesis of a nickel oxide/nickel heterostructural film for efficient hydrogen evolution reaction. *Chem Commun* 2020;56:10529-32. DOI
56. Wang P, Qin R, Ji P, et al. Synergistic coupling of Ni nanoparticles with Ni<sub>3</sub>C nanosheets for highly efficient overall water splitting. *Small* 2020;16:e2001642. DOI
57. Zhou P, Lv X, Gao Y, et al. Enhanced electrocatalytic HER performance of non-noble metal nickel by introduction of divanadium trioxide. *Electrochim Acta* 2019;320:134535. DOI
58. Sun J, Zhu M, Fan M, et al. Mo<sub>2</sub>C-Ni modified carbon microfibers as an effective electrocatalyst for hydrogen evolution reaction in acidic solution. *J Colloid Interface Sci* 2019;543:300-6. DOI
59. Yang L, Zhao X, Yang R, et al. In-situ growth of carbon nanotubes on Ni/NiO nanofibers as efficient hydrogen evolution reaction catalysts in alkaline media. *Appl Surface Sci* 2019;491:294-300. DOI
60. Barhoum A, El-Maghrabi HH, Iatsunskyi I, et al. Atomic layer deposition of Pd nanoparticles on self-supported carbon-Ni/NiO-Pd nanofiber electrodes for electrochemical hydrogen and oxygen evolution reactions. *J Colloid Interface Sci* 2020;569:286-97. DOI
61. Li T, Yin J, Sun D, et al. Manipulation of mott-schottky Ni/CeO<sub>2</sub> heterojunctions into N-doped carbon nanofibers for high-efficiency electrochemical water splitting. *Small* 2022;18:e2106592. DOI
62. Tao J, Zhang Y, Wang S, et al. Activating three-dimensional networks of Fe@Ni nanofibers via fast surface modification for efficient overall water splitting. *ACS Appl Mater Interfaces* 2019;11:18342-8. DOI
63. Zhang X, Wang J, Wang J, Wang J, Wang C, Lu C. Freestanding surface disordered NiCu solid solution as ultrastable high current density hydrogen evolution reaction electrode. *J Phys Chem Lett* 2021;12:11135-42. DOI
64. Li G, Wang J, Yu J, et al. Ni-Ni<sub>3</sub>P nanoparticles embedded into N, P-doped carbon on 3D graphene frameworks via in situ phosphatization of saccharomycetes with multifunctional electrodes for electrocatalytic hydrogen production and anodic degradation. *Appl Catal B Environ* 2020;261:118147. DOI
65. Jia D, Han L, Li Y, et al. Optimizing electron density of nickel sulfide electrocatalysts through sulfur vacancy engineering for alkaline hydrogen evolution. *J Mater Chem A* 2020;8:18207-14. DOI
66. Li YK, Zhang G, Lu WT, Cao FF. Amorphous Ni-Fe-Mo suboxides coupled with Ni network as porous nanoplate array on nickel foam: a highly efficient and durable bifunctional electrode for overall water splitting. *Adv Sci* 2020;7:1902034. DOI PubMed PMC
67. Liang W, Zhou M, Li X, et al. Oxygen-vacancy-rich MoO<sub>2</sub> supported nickel as electrocatalysts to promote alkaline hydrogen evolution and oxidation reactions. *Chem Eng J* 2023;464:142671. DOI
68. Mao B, Sun P, Jiang Y, et al. Identifying the transfer kinetics of adsorbed hydroxyl as a descriptor of alkaline hydrogen evolution reaction. *Angew Chem Int Ed* 2020;59:15232-7. DOI
69. Zhong W, Wang Z, Gao N, et al. Coupled vacancy pairs in Ni-doped CoSe for improved electrocatalytic hydrogen production through topochemical deintercalation. *Angew Chem Int Ed* 2020;59:22743-8. DOI
70. Jiao Y, Hong W, Li P, Wang L, Chen G. Metal-organic framework derived Ni/NiO micro-particles with subtle lattice distortions for high-performance electrocatalyst and supercapacitor. *Appl Catal B Environ* 2019;244:732-9. DOI

71. Tang Y, Liu Q, Dong L, Wu HB, Yu X. Activating the hydrogen evolution and overall water splitting performance of NiFe LDH by cation doping and plasma reduction. *Appl Catal B Environ* 2020;266:118627. DOI
72. Huang J, Han J, Wu T, et al. Boosting hydrogen transfer during volmer reaction at oxides/metal nanocomposites for efficient alkaline hydrogen evolution. *ACS Energy Lett* 2019;4:3002-10. DOI
73. Gu Y, Xi B, Wei R, Fu Q, Qain Y, Xiong S. Sponge assembled by graphene nanocages with double active sites to accelerate alkaline HER kinetics. *Nano Lett* 2020;20:8375-83. DOI
74. Xue S, Haid RW, Kluge RM, et al. Enhancing the hydrogen evolution reaction activity of platinum electrodes in alkaline media using nickel-iron clusters. *Angew Chem Int Ed* 2020;59:10934-8. DOI PubMed PMC
75. Tian Y, Huang A, Wang Z, et al. Two-dimensional hetero-nanostructured electrocatalyst of Ni/NiFe-layered double oxide for highly efficient hydrogen evolution reaction in alkaline medium. *Chem Eng J* 2021;426:131827. DOI
76. Suryanto BHR, Wang Y, Hocking RK, Adamson W, Zhao C. Overall electrochemical splitting of water at the heterogeneous interface of nickel and iron oxide. *Nat Commun* 2019;10:5599. DOI PubMed PMC
77. Sun H, Yan Z, Tian C, et al. Bixbyite-type  $\text{Ln}_2\text{O}_3$  as promoters of metallic Ni for alkaline electrocatalytic hydrogen evolution. *Nat Commun* 2022;13:3857. DOI PubMed PMC
78. Dastafkan K, Shen X, Hocking RK, Meyer Q, Zhao C. Monometallic interphasic synergy via nano-hetero-interfacing for hydrogen evolution in alkaline electrolytes. *Nat Commun* 2023;14:547. DOI PubMed PMC
79. Yang J, Shen Y, Sun Y, Xian J, Long Y, Li G. Ir nanoparticles anchored on metal-organic frameworks for efficient overall water splitting under pH-universal conditions. *Angew Chem Int Ed* 2023;62:e202302220. DOI
80. Bao J, Zhou Y, Zhang Y, et al. Engineering water splitting sites in three-dimensional flower-like Co-Ni-P/MoS<sub>2</sub> heterostructural hybrid spheres for accelerating electrocatalytic oxygen and hydrogen evolution. *J Mater Chem A* 2020;8:22181-90. DOI
81. Dai L, Chen ZN, Li L, Yin P, Liu Z, Zhang H. Ultrathin Ni(0)-embedded Ni(OH)<sub>2</sub> heterostructured nanosheets with enhanced electrochemical overall water splitting. *Adv Mater* 2020;32:e1906915. DOI
82. Zhong W, Li W, Yang C, et al. Interfacial electron rearrangement: Ni activated Ni(OH)<sub>2</sub> for efficient hydrogen evolution. *J Energy Chem* 2021;61:236-42. DOI
83. Tang Y, Dong L, Wu HB, Yu X. Tungstate-modulated Ni/Ni(OH)<sub>2</sub> interface for efficient hydrogen evolution reaction in neutral media. *J Mater Chem A* 2021;9:1456-62. DOI
84. Li J, Zhang Q, Zhang J, et al. Optimizing electronic structure of porous Ni/MoO<sub>2</sub> heterostructure to boost alkaline hydrogen evolution reaction. *J Colloid Interface Sci* 2022;627:862-71. DOI
85. Wu L, Zhang F, Song S, et al. Efficient alkaline water/seawater hydrogen evolution by a nanorod-nanoparticle-structured Ni-MoN catalyst with fast water-dissociation kinetics. *Adv Mater* 2022;34:e2201774. DOI
86. Zhang B, Du Z, Sun R, et al. Tremella-like Ni-NiO with O-vacancy heterostructure nanosheets grown in situ on MXenes for highly efficient hydrogen and oxygen evolution. *ACS Appl Mater Interfaces* 2022;14:47529-41. DOI
87. Zhou P, Tao L, Tao S, et al. Construction of nickel-based dual heterointerfaces towards accelerated alkaline hydrogen evolution via boosting multi-step elementary reaction. *Adv Funct Mater* 2021;31:2104827. DOI
88. Liu M, Sun Z, Zhang C, et al. Multi-interfacial engineering of a coil-like NiS-Ni<sub>2</sub>P/Ni hybrid to efficiently boost electrocatalytic hydrogen generation in alkaline and neutral electrolyte. *J Mater Chem A* 2022;10:13410-7. DOI
89. Liu M, Zou W, Cong J, Su N, Qiu S, Hou L. Identifying and unveiling the role of multivalent metal states for bidirectional UOR and HER over Ni, Mo-trithiocyanuric based coordination polymer. *Small* 2023;19:e2302698. DOI PubMed
90. Zhang J, Cui F, Ma Q, Cui T. Ni<sup>3+</sup>-rich Ni/NiO<sub>x</sub>@C nanocapsules below 4 nm constructed by low-temperature graphitization of self-assembled few-layer coordination polymers toward efficient alkaline hydrogen evolution electrocatalysis. *Small* 2024:e2311057. DOI PubMed
91. Kim J, Jung SM, Lee N, Kim KS, Kim YT, Kim JK. Efficient alkaline hydrogen evolution reaction using superaerophobic Ni nanoarrays with accelerated H<sub>2</sub> bubble release. *Adv Mater* 2023;35:e2305844. DOI
92. Xu X, Fu G, Wang Y, et al. Highly efficient all-3D-printed electrolyzer toward ultrastable water electrolysis. *Nano Lett* 2023;23:629-36. DOI
93. Fujimura T, Hikima W, Fukunaka Y, Homma T. Analysis of the effect of surface wettability on hydrogen evolution reaction in water electrolysis using micro-patterned electrodes. *Electrochem Commun* 2019;101:43-6. DOI
94. Shang L, Zhao Y, Kong X, et al. Underwater superaerophobic Ni nanoparticle-decorated nickel-molybdenum nitride nanowire arrays for hydrogen evolution in neutral media. *Nano Energy* 2020;78:105375. DOI
95. Li Y, Li J, Qian Q, et al. Superhydrophilic Ni-based multicomponent nanorod-confined-nanoflake array electrode achieves waste-battery-driven hydrogen evolution and hydrazine oxidation. *Small* 2021;17:e2008148. DOI
96. Gugtafeh HS, Rezaei M. Facile electrochemical synthesis of Ni-Sb nanostructure supported on graphite as an affordable bifunctional electrocatalyst for hydrogen and oxygen evolution reactions. *J. Electroanal Chem* 2022;922:116726. DOI
97. Yu W, Chen Z, Fu Y, et al. Superb all-pH hydrogen evolution performances powered by ultralow Pt-decorated hierarchical Ni-Mo porous microcolumns. *Adv Funct Mater* 2023;33:2210855. DOI
98. Jiang Y, Huang J, Mao B, An T, Wang J, Cao M. Inside solid-liquid interfaces: understanding the influence of the electrical double layer on alkaline hydrogen evolution reaction. *Appl Catal B Environ* 2021;293:120220. DOI
99. Zhang B, Zhang L, Tan Q, et al. Simultaneous interfacial chemistry and inner helmholtz plane regulation for superior alkaline hydrogen evolution. *Energy Environ Sci* 2020;13:3007-13. DOI

100. Gao L, Bao F, Tan X, et al. Engineering a local potassium cation concentrated microenvironment toward the ampere-level current density hydrogen evolution reaction. *Energy Environ Sci* 2023;16:285-94. [DOI](#)
101. Tan H, Tang B, Lu Y, et al. Engineering a local acid-like environment in alkaline medium for efficient hydrogen evolution reaction. *Nat Commun* 2022;13:2024. [DOI](#) [PubMed](#) [PMC](#)
102. Amaral L, Minkiewicz J, Šljukić B, et al. Toward tailoring of electrolyte additives for efficient alkaline water electrolysis: salicylate-based ionic liquids. *ACS Appl Energy Mater* 2018;1:4731-42. [DOI](#)
103. Amaral L, Minkiewicz J, Sljukic B, et al. Custom-made bromide-based ionic liquids as electrolyte additives for enhancing hydrogen evolution in alkaline water electrolysis. *J Electrochem Soc* 2019;166:1314. [DOI](#)